Mathematical Biosciences 000 (2015) 1–14

Contents lists available at ScienceDirect

Mathematical Biosciences

journal homepage: www.elsevier.com/locate/mbs

Analysis of a mathematical model for tumor therapy with a fusogenic oncolytic virus

Karly Jacobsen*, Sergei S. Pilyugin

Department of Mathematics, University of Florida, Gainesville, FL 32611, USA

ARTICLE INFO

Article history:
Revised 23 February 2015
Accepted 25 February 2015
Available online xxx

Keywords:
Oncolytic virus
Tumor
Syncytia
Hyperbolic–parabolic system
Free boundary problem

ABSTRACT

Oncolytic virotherapy is a tumor treatment which uses viruses to selectively target and destroy cancer cells. Fusogenic viruses, capable of causing cell-to-cell fusion upon infection of a tumor cell, have shown promise in experimental studies. Fusion causes the formation of large, multinucleated syncytia which eventually leads to cell death. We formulate a partial differential equations model with a moving boundary to describe the treatment of a spherical tumor with a fusogenic oncolytic virus. Fusion, lysis, and budding are incorporated as mechanisms of viral spread, resulting in nonlocal integral terms.

A proof is presented for existence and uniqueness of global solutions to the nonlinear hyperbolic–parabolic system. Numerical simulations demonstrate convergence to spatially homogeneous solutions and exponential growth or decay of the tumor radius depending on viral burst size and rate of fusion. Long-term tumor radius is shown to decrease with increasing values of viral burst size while the effect of the rate of fusion on tumor growth is demonstrated to be nonmonotonic.

1. Introduction

Tumor virotherapy uses replication-competent viruses which selectively infect, replicate in, and kill cancer cells. Commonly these viruses cause cell death through lysis; another mode of viral propagation is budding [1,2]. Clinical trials have demonstrated varying degrees of success for the therapy with limitations predominantly due to barriers to viral spread and the immune response to the virus [3].

A particularly interesting mechanism by which some oncolytic viruses act is through the formation of large, multinucleated cells called syncytia. When such a virus infects a tumor cell, the expression of fusogenic membrane glycoproteins on the surface of the cell allow for fusion with neighboring cells. The resulting syncytium will die by proteolytic digestion from within [4]. In this way, a significant bystander effect is created; experiments show that a single transfected cell can kill in excess of 150–200 bystander cells [5]. A measles vaccine strain, modified herpes simplex virus, and recombinant vesicular stomatitis virus have been shown to cause an increased cytopathic effect through the formation of syncytia [2,6,7]. The death of syncytia has also been shown to cause a potent antitumor immune response [2,4,8,9]. Thus, while demonstrating sufficient therapeutic efficacy remains a challenge for virotherapy, fusogenic oncolytic viruses hold promise for future clinical use.

Various mathematical models have been formulated to describe virotherapy treatment of tumors mediated by lysis [10–15]. The only models to our knowledge which consider syncytia formation are those by Bajzer and Dingli et al. [16–19]. Their deterministic models are formulated as ordinary differential equations which assume the law of mass action. However, a well-mixed tumor cell population is not biologically realistic and making this assumption may be obscuring relevant spatial effects. Our aim, therefore, is to develop a model for virotherapy with a fusogenic oncolytic virus which takes into account the inherent spatial dependency of syncytia-forming fusion. We also include lysis and budding, allowing the model to be tailored to a range of oncolytic viruses with differing viral spread mechanisms.

Section 2 describes the formulation of the model. A proof of well-posedness is given in Section 3. Numerical simulations and results are included in Section 4, followed by a brief discussion in Section 5.

2. Formulation of the model

We adapt a similar setup to the partial differential equations models of Wu et al. [10] and Friedman et al. [13] but also incorporate cell-to-cell fusion. We allow for viral budding from infected and syncytia-incorporated cells as well as viral diffusion but neglect necrosis to improve mathematical tractability. We assume that the tumor is spherically symmetric with radius $R(t)$. We let $x(r, t)$ be the density of uninfected tumor cells whose center is a distance r from

* Corresponding author. Present address: Mathematical Biosciences Institute, The Ohio State University, 1735 Neil Avenue, Columbus, OH 43210, USA. Tel.: +1 614 688 3198.

E-mail addresses: jacobsen.50@mbi.osu.edu (K. Jacobsen), pilyugin@ufl.edu (S.S. Pilyugin).

http://dx.doi.org/10.1016/j.mbs.2015.02.009
0025-5564/

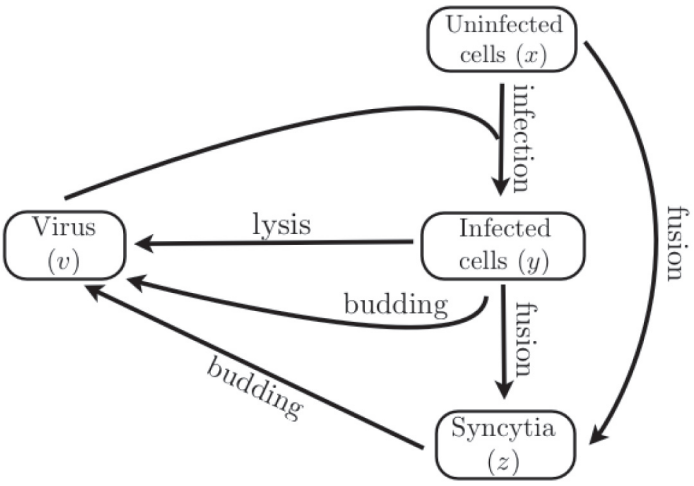

Fig. 1. Model interaction network. Uninfected tumor cells become infected upon entry of a free virus. Infected cells undergo lysis resulting in release of free viruses. Uninfected and infected cells can fuse with neighboring cells to become syncytia. Infected cells and syncytia release free viruses via budding.

the center of the tumor. Similarly, $y(r, t)$ and $z(r, t)$ represent the density of infected tumor cells and syncytia-incorporated cells, respectively. We assume that all tumor cells are spherical with radius r_c. We let $v(r, t)$ be the density of free viral particles which we assume have negligible volume. We model the tumor as an incompressible fluid under an advective field velocity $u(r, t)$.

The dynamics of the tumor cell and virus populations are based on the network shown in Fig. 1. We suppose that only uninfected cells proliferate, at a rate λ. Uninfected cells become infected at a rate that is proportional to the average number of viral particles on the surface of the cell. The coefficient of proportionality, β, takes into the account the probability of success of viral entry. The derivation of the corresponding integral expression in Eqs. (1) and (2) will be discussed in Section 2.2. We make the simplifying assumption that a cell which is syncytia-incorporated is still spherical with radius r_c. An uninfected cell can fuse into a syncytia if it is in contact with either an infected cell or a syncytia-incorporated cell. We assume this fusion occurs at a rate with coefficient ρ and is proportional to the average density of neighboring infected and syncytia-incorporated cells. We will derive in Section 2.2 the exact formulation of the corresponding integral term in Eqs. (1) and (3). A single infected cell can be incorporated into a syncytia through surface contact with a cell of any other type, again at a rate proportional to ρ. Since we neglect necrosis we assume that immediately upon death a cell is removed. For infected cells this process occurs at rate δ and for syncytia at rate μ.

We allow free viral particles to be generated through two mechanisms, budding and lysis. An infected or syncytia-incorporated cell releases viral particles from their surface through budding at a rate α. It is hypothesized that syncytia are removed via a non-apoptotic mechanism that doesn't allow viral release [4]. Therefore we assume that only infected cells undergo lysis upon death, releasing N viral particles. More detail on the corresponding budding and lysis terms in Eq. (4) is discussed in Section 2.2. We further assume that free viral particles are removed at rate γ.

Therefore, for $0 < r \le R(t)$ and $t > 0$, the dynamics of the state variables are determined by

$$\begin{aligned}\frac{Dx}{Dt} &\equiv \frac{\partial x(r,t)}{\partial t} + \frac{1}{r^2}\frac{\partial}{\partial r}(r^2 u(r,t)x(r,t)) \\ &= \lambda x(r,t) - \frac{\beta x(r,t)}{|I_{r_c}(r,t)|}\int_{I_{r_c}(r,t)} v(s,t)\,ds \\ &\quad - \frac{\rho x(r,t)}{|I_{2r_c}(r,t)|}\int_{I_{2r_c}(r,t)} y(s,t) + z(s,t)\,ds, \end{aligned} \tag{1}$$

$$\begin{aligned}\frac{Dy}{Dt} &\equiv \frac{\partial y(r,t)}{\partial t} + \frac{1}{r^2}\frac{\partial}{\partial r}(r^2 u(r,t)y(r,t)) \\ &= \frac{\beta x(r,t)}{|I_{r_c}(r,t)|}\int_{I_{r_c}(r,t)} v(s,t)\,ds - (\rho\theta + \delta)y(r,t), \end{aligned} \tag{2}$$

$$\begin{aligned}\frac{Dz}{Dt} &\equiv \frac{\partial z(r,t)}{\partial t} + \frac{1}{r^2}\frac{\partial}{\partial r}(r^2 u(r,t)z(r,t)) \\ &= \frac{\rho x(r,t)}{|I_{2r_c}(r,t)|}\int_{I_{2r_c}(r,t)} y(s,t) + z(s,t)\,ds + \rho\theta y(r,t) - \mu z(r,t), \end{aligned} \tag{3}$$

$$\begin{aligned}&\frac{\partial v(r,t)}{\partial t} - \kappa\frac{1}{r^2}\frac{\partial}{\partial r}\left(r^2\frac{\partial v(r,t)}{\partial r}\right) \\ &\quad = \frac{N\delta}{|J_{r_c}(r,t)|}\int_{I_{r_c}(r,t)}\left[r_c^2 - (r-s)^2\right]y(s,t)\,ds \\ &\qquad + \frac{\alpha}{|I_{r_c}(r,t)|}\int_{I_{r_c}(r,t)} y(s,t) + z(s,t)\,ds - \gamma v(r,t) \end{aligned} \tag{4}$$

where $I_{r_c}(r, t) = (\max[0, r - r_c], \min[R(t), r + r_c])$ and

$$|J_{r_c}(r,t)| = \int_{I_{r_c}(r,t)}\left[r_c^2 - (r-s)^2\right]ds.$$

The last term on the left-hand side in each of Eqs. (1), (2), and (3) corresponds to advection. Note that the viral particles, being of negligible volume, do not undergo advection but do diffuse with diffusion coefficient κ.

Treating the tumor as an incompressible fluid, we assume that the total tumor cell density has a constant value θ. That is,

$$x(r,t) + y(r,t) + z(r,t) = \theta \tag{5}$$

for $0 < r \le R(t)$. Therefore summing Eqs. (1), (2) and (3) gives

$$\frac{\theta}{r^2}\frac{\partial}{\partial r}(r^2 u(r,t)) = \lambda x(r,t) - \delta y(r,t) - \mu z(r,t). \tag{6}$$

Then the advection term, in Eq. (1) for example, by the product rule becomes

$$\begin{aligned}\frac{-1}{r^2}\frac{\partial}{\partial r}(r^2 u(r,t)x(r,t)) &= -u(r,t)\frac{\partial x(r,t)}{\partial r} \\ &\quad - \frac{x(r,t)}{\theta}[\lambda x(r,t) - \delta y(r,t) - \mu z(r,t)].\end{aligned}$$

By Eq. (5) we have $z = \theta - x - y$ and we can reduce the dimension of the system. By integrating Eq. (6) and eliminating z, we present the first complete formulation of our model. For $0 < r \le R(t)$ and $t > 0$,

$$\begin{aligned}&\frac{\partial x(r,t)}{\partial t} + u(r,t)\frac{\partial x(r,t)}{\partial r} = \lambda x(r,t) - \frac{\beta x(r,t)}{|I_{r_c}(r,t)|}\int_{I_{r_c}(r,t)} v(s,t)\,ds \\ &\quad - \frac{\rho x(r,t)}{|I_{2r_c}(r,t)|}\int_{I_{2r_c}(r,t)} \theta - x(s,t)\,ds \\ &\quad - \frac{x(r,t)}{\theta}[\lambda x(r,t) - \delta y(r,t) - \mu(\theta - x(r,t) - y(r,t))], \end{aligned} \tag{7}$$

$$\begin{aligned}&\frac{\partial y(r,t)}{\partial t} + u(r,t)\frac{\partial y(r,t)}{\partial r} \\ &\quad = \frac{\beta x(r,t)}{|I_{r_c}(r,t)|}\int_{I_{r_c}(r,t)} v(s,t)\,ds - (\rho\theta + \delta)y(r,t) \\ &\quad - \frac{y(r,t)}{\theta}[\lambda x(r,t) - \delta y(r,t) - \mu(\theta - x(r,t) - y(r,t))], \end{aligned} \tag{8}$$

$$\begin{aligned}&\frac{\partial v(r,t)}{\partial t} - \kappa\frac{1}{r^2}\frac{\partial}{\partial r}\left(r^2\frac{\partial v(r,t)}{\partial r}\right) \\ &\quad = \frac{N\delta}{|J_{r_c}(r,t)|}\int_{I_{r_c}(r,t)}\left[r_c^2 - (r-s)^2\right]y(s,t)\,ds \\ &\qquad + \frac{\alpha}{|I_{r_c}(r,t)|}\int_{I_{r_c}(r,t)} \theta - x(s,t)\,ds - \gamma v(r,t), \end{aligned} \tag{9}$$

Please cite this article as: K. Jacobsen, S. S. Pilyugin, Analysis of a mathematical model for tumor therapy with a fusogenic oncolytic virus, Mathematical Biosciences (2015), http://dx.doi.org/10.1016/j.mbs.2015.02.009

$$u(r,t) = \frac{1}{\theta r^2}\int_0^r s^2[-\mu\theta + (\lambda+\mu)x(s,t) + (\mu-\delta)y(s,t)]\,ds, \quad (10)$$

$$\frac{dR(t)}{dt} = u(R(t),t). \quad (11)$$

We assume a Stefan, or moving, boundary condition which gives Eq. (11); the radius of the tumor $R(t)$ is changing at exactly the rate of the local advective velocity.

2.1. Boundary and initial conditions

The boundary conditions at the tumor center,

$$\frac{\partial x(r,t)}{\partial r} = \frac{\partial y(r,t)}{\partial r} = \frac{\partial v(r,t)}{\partial r} = u(r,t) = 0 \qquad \text{at} \qquad r = 0, \quad (12)$$

follow from radial symmetry. We additionally assume the Neumann boundary condition

$$\frac{\partial v(r,t)}{\partial r} = 0 \qquad \text{at} \qquad r = R(t). \quad (13)$$

In Section 2.3, we will make a transformation to fix the moving boundary and no other conditions will be needed at the tumor boundary.

The initial conditions are given by

$$\tilde{x}(r,0) = \tilde{x}_0(r), \quad \tilde{y}(r,0) = \tilde{y}_0(r), \quad \tilde{v}(r,0) = \tilde{v}_0(r), \quad R(0) = R_0 \quad (14)$$

for $0 \le r \le R(t)$ where $\tilde{x}_0(r) \ge 0, \tilde{y}_0(r) \ge 0, \tilde{x}_0(r) + \tilde{y}_0(r) \le \theta, \tilde{v}_0(r) \ge 0, R_0 > 0$ and $\tilde{x}_0(r), \tilde{y}_0(r)$ and $\tilde{v}_0(r)$ are continuously differentiable functions on $[0, R_0]$.

2.2. Derivation of nonlocal integral terms

Wu et al. describe in detail the formulation of similar integral terms for infection and lysis where, instead, the limits of integration are $r - r_c$ and $r + r_c$ [10] . However, here we acknowledge the necessity of $I_{r_c}(r,t)$ and $J_{r_c}(r,t)$, as defined in Section 2, to maintain the well-posedness of the model by ensuring that the limits of integration are within the physical bounds of the tumor. We adopt their notation and likewise construct local spherical $(\tilde{r}, \tilde{\theta}, \tilde{\phi})$, Cartesian $(\tilde{x}, \tilde{y}, \tilde{z})$, and cylindrical $(\tilde{\rho}, \tilde{\theta}, \tilde{z})$ coordinates with the $\tilde{z}$ axis parallel to the radial direction s of the tumor (Fig. 2).

For the term describing the fusion of an uninfected cell at a radial distance r from the tumor center, we seek to find $\overline{w}_{2r_c}(r,t)$, the spatially-weighted average of its neighboring infected and syncytia-incorporated cells. We observe that cells are "neighboring" if and only if the distance between their centers is exactly $2r_c$ (Fig. 3(a)). Let $W_{2r_c}(r,t)$ be its total number of neighboring infected and syncytia-incorporated cells. It holds that $s = r + \tilde{z}$, $ds = d\tilde{z}$, $\tilde{z} = 2r_c\cos\tilde{\phi}$, and $d\tilde{z} = -2r_c\sin\tilde{\phi}\,d\tilde{\phi}$.

Let $I_{\min} = \min(I_{2r_c}(r,t))$ and $I_{\max} = \max(I_{2r_c}(r,t))$. Subsequently, we define $a = \arccos((I_{\max} - r)/2r_c)$ and $b = \arccos((I_{\min} - r)/2r_c)$. Since $0 \le \tilde{\phi} \le 2\pi$, it follows that $a \le b$. Therefore we calculate that

$$\begin{aligned} W_{2r_c}(r,t) &= \int_0^{2\pi}\int_a^b \left(y(r+\tilde{z},t) + z(r+\tilde{z},t)\right)(2r_c)^2\sin\tilde{\phi}\,d\tilde{\phi}\,d\tilde{\theta} \\ &= 8\pi r_c^2\int_a^b \left(y(r+\tilde{z},t) + z(r+\tilde{z},t)\right)\sin\tilde{\phi}\,d\tilde{\phi} \\ &= 4\pi r_c\int_{I_{\min}-r}^{I_{\max}-r} \left(y(r+\tilde{z},t) + z(r+\tilde{z},t)\right)\,d\tilde{z} \\ &= 4\pi r_c\int_{I_{\min}}^{I_{\max}} \left(y(s,t) + z(s,t)\right)\,ds \\ &= 4\pi r_c\int_{I_{2r_c}(s,t)} \left(\theta - x(s,t)\right)\,ds. \end{aligned}$$

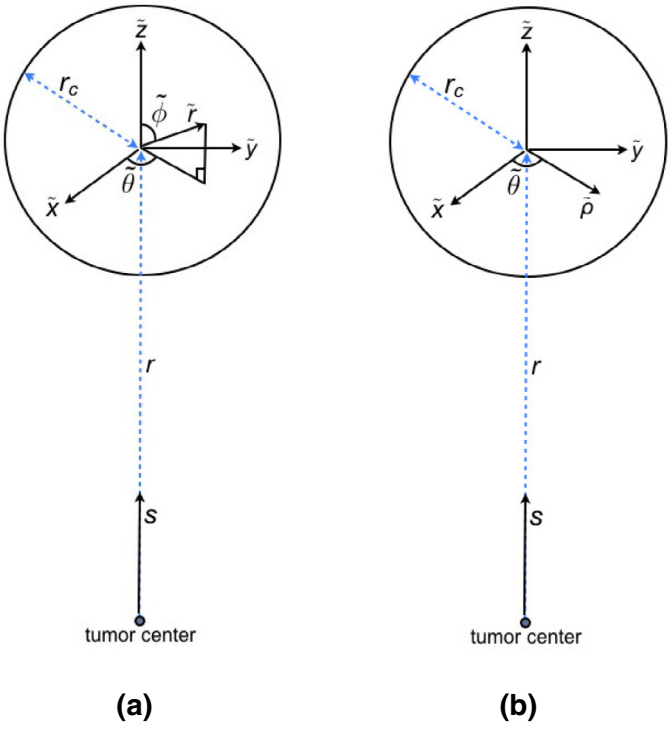

Fig. 2. Local coordinate systems with their origins at the center of a tumor cell a distance r from the tumor center. (a) Spherical $(\tilde{r}, \tilde{\theta}, \tilde{\phi})$ and Cartesian $(\tilde{x}, \tilde{y}, \tilde{z})$. (b) Cylindrical $(\tilde{\rho}, \tilde{\theta}, \tilde{z})$ and Cartesian $(\tilde{x}, \tilde{y}, \tilde{z})$. See also [10].

Likewise, the total surface area, $A_{2r_c}(r,t)$, of integration is

$$A_{2r_c}(r,t) = \int_0^{2\pi}\int_a^b (2r_c)^2\sin\tilde{\phi}\,d\tilde{\phi}\,d\tilde{\theta} = 4\pi r_c|I_{2r_c}(r,t)|.$$

The spatially-weighted average $\overline{w}_{2r_c}(r,t)$ is then given by

$$\frac{W_{2r_c}(r,t)}{A_{2r_c}(r,t)} = \frac{1}{|I_{2r_c}(r,t)|}\int_{I_{2r_c}(r,t)} \left(\theta - x(s,t)\right)\,ds.$$

Hence we obtain the integral term for fusion in Eq. (7). Note that, because we assume infected cells can form syncytia with any other type of cell, the analogous rate of fusion for infected cells in Eq. (8) reduces to $\rho\theta$.

A free viral particle generated by budding at a distance r from the tumor center must be released from an infected cell or syncytia-incorporated cell that is a distance r_c away (Fig. 3(b)). Therefore, the term in Eq. (9) for budding can be derived similarly. Likewise, the infection of a tumor cell occurs by the presence of a free viral particle on the surface of the cell, i.e. at a distance r_c away from the cell center (Fig. 3(c)), so the integral term for infection in Eq. (7) follows analogously.

We assume that lysis of an infected cell releases free viral particles uniformly throughout the volume of the cell. So if a free viral particle is generated by lysis at a distance r from the tumor center, then it must have been released from an infected cell whose center is less than or equal to r_c away from it (Fig. 3(d)). Hence, to derive the lysis integral term, we consider the spatially-weighted volume average, $\overline{y}_{r_c}(r,t)$, of infected cells within a distance r_c from the viral particle. Let

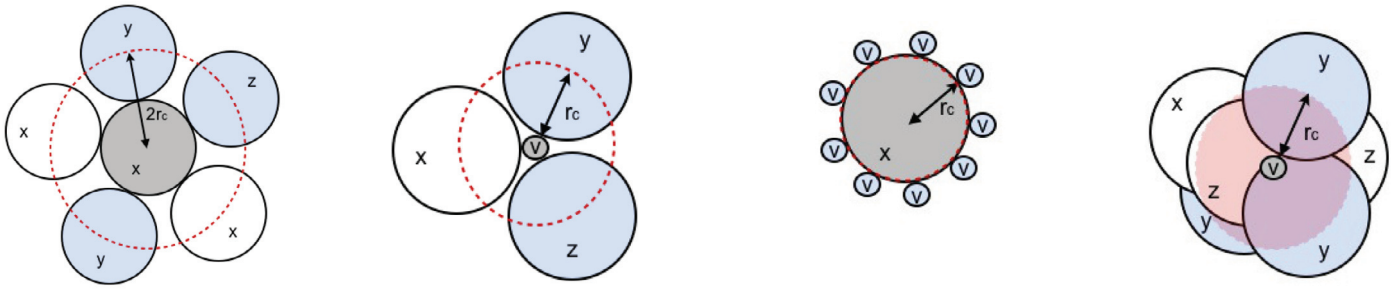

(a) Fusion (b) Budding (c) Infection (d) Lysis

Fig. 3. Schematic drawings of the cell arrangements pertaining to derivation of the integral terms for fusion (a), viral budding (b), viral infection (c), and lysis (d). For a cell of interest (gray), the derivation includes the appropriate cells (blue) that are a prescribed distance away (red). Cell types indicated are uninfected cells (x), infected cells (y), and syncytia-incorporated cells (z). v represents a free viral particle. (For interpretation of the references to color in this figure legend, the reader is referred to the web version of this article.)

$i_{\min} = \min(I_{r_c}(r,t))$ and $i_{\max} = \max(I_{r_c}(r,t))$. Using the cylindrical coordinates (Fig. 2(b)), we calculate $Y_{r_c}(r,t)$, the total number of infected cells within a distance r_c from the viral particle, to be

$$\begin{aligned} Y_{r_c}(r,t) &= \int_0^{2\pi}\int_{i_{\min}-r}^{i_{\max}-r}\int_0^{\sqrt{r_c^2-\tilde z^2}} y(r+\tilde z,t)\tilde\rho\, d\tilde\rho\, d\tilde z\, d\tilde\theta \\ &= \pi\int_{i_{\min}-r}^{i_{\max}-r}\left(r_c^2-\tilde z^2\right) y(r+\tilde z,t)\, d\tilde z \\ &= \pi\int_{I_{r_c}(r,t)}\left[r_c^2-(s-r)^2\right] y(s,t)\, ds. \end{aligned}$$

The total volume $V_{r_c}(r,t)$ of integration is

$$\begin{aligned} V_{r_c}(r,t) &= \int_0^{2\pi}\int_{i_{\min}-r}^{i_{\max}-r}\int_0^{\sqrt{r_c^2-\tilde z^2}} \tilde\rho\, d\tilde\rho\, d\tilde z\, d\tilde\theta \\ &= \pi\int_{I_{r_c}(r,t)}\left[r_c^2-(s-r)^2\right] ds = \pi\,|J_{r_c}(r,t)|. \end{aligned}$$

Therefore,

$$\bar y_{r_c}(r,t) = \frac{Y_{r_c}(r,t)}{V_{r_c}(r,t)} = \frac{1}{|J_{r_c}(r,t)|}\int_{I_{r_c}(r,t)}\left[r_c^2-(s-r)^2\right] y(s,t)\, ds$$

from which the lysis term in Eq. (9) follows.

2.3. Transformation of the system

Before proving the main existence and uniqueness result of Section 3 we will perform a transformation to the system (7)–(14) in order to fix the moving boundary. The now routine transformation was first introduced by Landau [20]. We define new space and time variables, $\sigma(r,t) := r/R(t)$ and $\tau(r,t) := t$. We observe that

$$\frac{\partial\sigma}{\partial r} = \frac{1}{R(t)} \quad\text{and}\quad \frac{\partial\sigma}{\partial\tau} = \frac{\partial\sigma}{\partial t}\cdot\frac{\partial t}{\partial\tau} = \frac{-r}{(R(t))^2}\frac{dR(t)}{dt} = \frac{-\sigma}{R(\tau)}\frac{dR(\tau)}{d\tau}.$$

We define $\tilde x(\sigma,\tau) := x(\sigma(r,t)R(t),t)$ and let $\tilde y(\sigma,\tau), \tilde v(\sigma,\tau)$, and $\tilde u(\sigma,\tau)$ be defined similarly. Then it follows that

$$\frac{\partial x(r,t)}{\partial t} = \frac{\partial\tilde x(\sigma,\tau)}{\partial\sigma}\cdot\frac{\partial\sigma}{\partial t} + \frac{\partial\tilde x(\sigma,\tau)}{\partial\tau}\cdot\frac{\partial\tau}{\partial t}.$$

Therefore

$$\begin{aligned} \frac{\partial\tilde x(\sigma,\tau)}{\partial\tau} &= \frac{\partial x(r,t)}{\partial t} - \frac{\partial\tilde x(\sigma,\tau)}{\partial\sigma}\cdot\frac{\partial\sigma}{\partial t} \\ &= \frac{\partial x(r,t)}{\partial t} + \frac{\sigma}{R(\tau)}\cdot\frac{dR(\tau)}{d\tau}\cdot\frac{\partial\tilde x(\sigma,\tau)}{\partial\sigma}. \end{aligned} \tag{15}$$

Similarly, Eq. (15) holds for $\tilde y$ and $\tilde v$. Transformation of the integral terms requires the definition of $I_{r_c}(\sigma,\tau) = (\max[0,\sigma - r_c/R(\tau)], \min[1,\sigma + r_c/R(\tau)])$ and $|J_{r_c}(\sigma,\tau)| = \int_{I_{r_c}(\sigma,\tau)}[r_c^2 - R^2(\tau)(\omega-\sigma)^2]\, d\omega$. Therefore the transformed model becomes, for $\sigma\in(0,1]$ and $\tau>0$,

$$\begin{aligned} &\frac{\partial\tilde x(\sigma,\tau)}{\partial\tau} + \left[-\frac{\sigma}{R(\tau)}\frac{dR(\tau)}{d\tau} + \frac{\tilde u(\sigma,\tau)}{R(\tau)}\right]\frac{\partial\tilde x(\sigma,\tau)}{\partial\sigma} \\ &= \lambda\tilde x(\sigma,\tau) - \frac{\beta\tilde x(\sigma,\tau)}{|I_{r_c}(\sigma,\tau)|}\int_{I_{r_c}(\sigma,\tau)}\tilde v(\omega,\tau)\, d\omega \\ &\quad - \frac{\rho\tilde x(\sigma,\tau)}{|I_{2r_c}(\sigma,\tau)|}\int_{I_{2r_c}(\sigma,\tau)}\theta - \tilde x(\omega,\tau)\, d\omega \\ &\quad - \frac{\tilde x(\sigma,\tau)}{\theta}[\lambda\tilde x(\sigma,\tau) - \delta\tilde y(\sigma,\tau) - \mu(\theta - \tilde x(\sigma,\tau) - \tilde y(\sigma,\tau)], \end{aligned} \tag{16}$$

$$\begin{aligned} &\frac{\partial\tilde y(\sigma,\tau)}{\partial\tau} + \left[-\frac{\sigma}{R(\tau)}\frac{dR(\tau)}{d\tau} + \frac{\tilde u(\sigma,\tau)}{R(\tau)}\right]\frac{\partial\tilde y(\sigma,\tau)}{\partial\sigma} \\ &= \frac{\beta\tilde x(\sigma,\tau)}{|I_{r_c}(\sigma,\tau)|}\int_{I_{r_c}(\sigma,\tau)}\tilde v(\omega,\tau)\, d\omega - (\rho\theta+\delta)\tilde y(\sigma,\tau) \\ &\quad - \frac{\tilde y(\sigma,\tau)}{\theta}[\lambda\tilde x(\sigma,\tau) - \delta\tilde y(\sigma,\tau) - \mu(\theta - \tilde x(\sigma,\tau) - \tilde y(\sigma,\tau)], \end{aligned} \tag{17}$$

$$\begin{aligned} &\frac{\partial\tilde v(\sigma,\tau)}{\partial\tau} - \frac{\sigma}{R(\tau)}\frac{dR(\tau)}{d\tau}\frac{\partial\tilde v(\sigma,\tau)}{\partial\sigma} - \frac{\kappa}{R^2(\tau)}\frac{1}{\sigma^2}\frac{\partial}{\partial\sigma}\left(\sigma^2\frac{\partial\tilde v(\sigma,\tau)}{\partial\sigma}\right) \\ &= \frac{N\delta}{|J_{r_c}(\sigma,\tau)|}\int_{I_{r_c}(\sigma,\tau)}[r_c^2 - R^2(\tau)(\sigma-\omega)^2]\tilde y(\omega,\tau)\, d\omega \\ &\quad + \frac{\alpha}{|I_{r_c}(\sigma,\tau)|}\int_{I_{r_c}(\sigma,\tau)}\theta - \tilde x(\omega,\tau)\, d\omega - \gamma\tilde v(\sigma,\tau), \end{aligned} \tag{18}$$

$$\begin{aligned} \tilde u(\sigma,\tau) = \frac{R(\tau)}{\theta\sigma^2}\int_0^\sigma \omega^2[&-\mu\theta + (\lambda+\mu)\tilde x(\omega,\tau) \\ &+(\mu-\delta)\tilde y(\omega,\tau)]\, d\omega, \end{aligned} \tag{19}$$

$$\frac{dR(\tau)}{d\tau} = \tilde u(1,\tau). \tag{20}$$

The boundary and initial conditions are given, for $\tau>0$, by

$$\frac{\partial\tilde v}{\partial\sigma}(0,\tau) = \frac{\partial\tilde v}{\partial\sigma}(1,\tau) = 0, \tag{21}$$

$$\tilde v(\sigma,0) = \tilde v_0(\sigma) \quad\text{for}\quad 0\le\sigma\le 1, \tag{22}$$

$$\frac{\partial\tilde x}{\partial\sigma}(0,\tau) = \frac{\partial\tilde y}{\partial\sigma}(0,\tau) = 0 \tag{23}$$

$$\tilde x(\sigma,0) = \tilde x_0(\sigma), \quad \tilde y(\sigma,0) = \tilde y_0(\sigma) \quad\text{for}\quad 0\le\sigma\le 1. \tag{24}$$

$$\tilde u(0,\tau) = 0, \tag{25}$$

$$R(0) = R_0. \tag{26}$$

We additionally will assume that $\tilde x_0(\sigma)\ge 0, \tilde y_0(\sigma)\ge 0, \tilde x_0(\sigma) + \tilde y_0(\sigma)\le\theta, \tilde v_0(\sigma)\ge 0, R_0>0$, $\frac{\partial\tilde x}{\partial\sigma}(0) = \frac{\partial\tilde y}{\partial\sigma}(0) = \frac{\partial\tilde v}{\partial\sigma}(0) = \frac{\partial\tilde v}{\partial\sigma}(1) = 0$

and that $\tilde{x}_0(\sigma), \tilde{y}_0(\sigma)$, and $\tilde{v}_0(\sigma)$ are continuously differentiable functions on $[0, 1]$.

We note that when $\sigma = 1$ the coefficient of $\frac{\partial \tilde{x}(\sigma,\tau)}{\partial \sigma}$ in Eq. (16) is $[-dR(\tau)/d\tau + \tilde{u}(1,\tau)]/R(\tau)$ which by Eq. (20) is zero. Thus we do not need to impose a boundary condition for $\frac{\partial \tilde{x}(1,\tau)}{\partial \sigma}$. The same justification holds for $\frac{\partial \tilde{y}(1,\tau)}{\partial \sigma}$.

3. Existence and uniqueness of solutions

The main result of this section establishes the existence and uniqueness of global solutions to the system (16)–(26). Friedman and Tao proved existence and uniqueness of solutions to a simpler model for oncolytic virotherapy [13]. The general structure of the proof presented here, as a nested application of the Contraction Mapping Theorem, follows that by Friedman and Tao. However, our model requires further significant considerations which arise from the nonlocal integral terms and the additional coupling of equations due to fusion and budding.

We begin by defining two complete metric spaces of functions. Lemma 1 then establishes the existence of a solution to the parabolic system (18), (21), (22) given fixed $\tilde{u}, \tilde{x}$, and $\tilde{y}$. Lemma 2, on the other hand, provides a solution to the hyperbolic system (16), (17), (23), (24) for fixed $\tilde{u}$ and $\tilde{v}$.

3.1. Preliminary definitions

We use $\|\cdot\|$ throughout to denote the sup norm. That is, for a function $f : X \to \mathbb{R}$, we let $\|f\| = \sup_{x\in X} |f(x)|$ and for $f : X \to \mathbb{R}^2$, given by $x \to (f_1(x), f_2(x))$, we let $\|f\| = \max(\|f_1\|, \|f_2\|)$.

For $T > 0$ we consider the complete metric space of functions $E_T \subset C([0, 1] \times [0, T])$ given by

$$E_T = \{\tilde{u}(\sigma,\tau) \in C([0,1]\times[0,T]) : \tilde{u}(0,\tau) = 0, \tilde{u}(\sigma,0) = \tilde{u}_0(\sigma), \|\tilde{u}\| \le L, |\tilde{u}(\sigma_1,\tau) - \tilde{u}(\sigma_2,\tau)| \le K|\sigma_1 - \sigma_2| \text{ for all } \sigma,\sigma_1,\sigma_2 \in [0,1], \tau \in [0,T]\},$$

where

$$L > R_0 \cdot \max\left(\frac{\mu+\delta}{3}, \frac{\lambda}{3}\right), \quad K \ge 5L\left(1 + \frac{TL}{R_0}\right), \tag{27}$$

and

$$\tilde{u}_0(\sigma) = \frac{R_0}{\theta\sigma^2}\int_0^\sigma \omega^2[-\mu\theta + (\lambda+\mu)\tilde{x}_0(\omega) + (\mu-\delta)\tilde{y}_0(\omega)]\,d\omega.$$

We note that E_T is nonempty since $\tilde{u}(\sigma,\tau) \equiv \tilde{u}_0(\sigma) \in E_T$. For a given $\tilde{u} \in E_T$ we define $R(\tau)$ by

$$R(\tau) = R_0 + \int_0^\tau \tilde{u}(1,s)\,ds. \tag{28}$$

We observe that for, any $\tilde{u} \in E_T$,

$$0 < R_0 - TL \le R(\tau) \le R_0 + TL \tag{29}$$

if T is sufficiently small. Hence Eq. (28) and inequality (29) imply that

$$\left|\frac{1}{R(\tau)}\cdot\frac{dR(\tau)}{d\tau}\right| \le \frac{L}{R_0 - LT}. \tag{30}$$

Fix $\tilde{u} \in E_T$. Let $\xi(\tau;\sigma,s)$ be the backward characteristic curve of Eqs. (16), (17) such that $\xi|_{\tau=s} = \sigma$. That is, for $0 \le \tau \le s$,

$$\begin{cases} \dfrac{d\xi}{d\tau} = -\dfrac{\xi}{R(\tau)}\dfrac{dR(\tau)}{d\tau} + \dfrac{\tilde{u}(\xi,\tau)}{R(\tau)} \\ \xi(s;\sigma,s) = \sigma. \end{cases} \tag{31}$$

The existence and uniqueness of ξ for every $(\sigma, s) \in [0, 1] \times [0, T]$ follows from a standard theorem of ordinary differential equations since the right hand side of Eq. (31) is continuous and Lipschitz with respect to ξ and continuous with respect to τ [21, Theorem 1.261, page 138]. Note that $\xi \equiv 0$ is a characteristic since $\tilde{u}(0,\tau) = 0$ and $\xi \equiv 1$ is also a characteristic by Eq. (28). Thus by uniqueness,

$$0 < \xi(\tau;\sigma,s) < 1 \tag{32}$$

for any $(\sigma, s) \in (0, 1) \times [0, T]$. We will suppress two arguments and use the notation $\xi(\tau) = \xi(\tau;\sigma,s)$. For $T > 0$ we also will consider the complete metric space of pairs of functions given by

$$S_T = \{(x(\xi(\tau),\tau), y(\xi(\tau),\tau)) : x(\xi(\tau),\tau), y(\xi(\tau),\tau) \in C[0,T], 0 \le x(\xi(\tau),\tau) \le \theta, 0 \le y(\xi(\tau),\tau) \le \theta\}.$$

We must make one final observation which is that $|I_{r_c}(\xi(\tau),\tau)|$, the length of the interval $I_{r_c}(\xi(\tau),\tau)$, is uniformly bounded above and below. Indeed, a straightforward calculation from the definition of $I_{r_c}(\xi(\tau),\tau)$, recalling inequalities (29) and (32), yields that for any $\tau \in [0, T]$ and $\xi \in [0, 1]$

$$\min\left(1, \frac{r_c}{R_0 + TL}\right) \le |I_{r_c}(\xi(\tau),\tau)| \le \max\left(\frac{2r_c}{R_0 - TL}, 1 + \frac{r_c}{R_0 - TL}\right). \tag{33}$$

3.2. Existence and uniqueness for the parabolic and hyperbolic subsystems

Lemma 1. *Consider $(\hat{x}, \hat{y}) \in S_T$. Then there exists a unique, continuous solution $\tilde{v}$ to the system (18), (21), (22) with $\hat{x}$ and $\hat{y}$ replacing $\tilde{x}$ and $\tilde{y}$, respectively. Furthermore, for any $(\sigma,\tau) \in [0,1]\times[0,T]$*

$$0 \le \tilde{v}(\sigma,\tau) \le \max[(N\delta + \alpha)\theta/\gamma, \|\tilde{v}_0\|]. \tag{34}$$

Proof. We define the parabolic operator

$$L\tilde{v} = \frac{\kappa}{R^2(\tau)}\frac{\partial^2\tilde{v}}{\partial\sigma^2} + \left[\frac{2\kappa}{\sigma} + \frac{\sigma}{R(\tau)}\frac{dR(\tau)}{d\tau}\right]\frac{\partial\tilde{v}}{\partial\sigma} - \gamma\tilde{v} - \frac{\partial\tilde{v}}{\partial\tau}$$

and the function

$$f(\sigma,\tau) = \frac{N\delta}{|I_{r_c}(\sigma,\tau)|}\int_{I_{r_c}(\sigma,\tau)}\left[r_c^2 - R^2(\tau)(\sigma-\omega)^2\right]\hat{y}(\omega,\tau)\,d\omega + \frac{\alpha}{|I_{r_c}(\sigma,\tau)|}\int_{I_{r_c}(\sigma,\tau)}\theta - \hat{x}(\omega,\tau)\,d\omega.$$

Then Eq. (18) is equivalent to $L\tilde{v} + f(\sigma,\tau) = 0$ for any solution $\tilde{v}$ to Eq. (18). If we convert to Cartesian coordinates, we see that all the coefficients of the parabolic operator are bounded, and thus the existence and uniqueness of a classical solution $\tilde{v}$ follows from standard parabolic theory [22, Theorem 2, page 144].

Furthermore, we note that the coefficients of the operator L are bounded on every closed ball contained in $(0, 1] \times [0, T]$ and $f(\sigma,\tau) \ge 0$ since $\hat{y} \ge 0$ and $\hat{x} \le \theta$. Therefore the parabolic comparison principle [23, Theorem 1.2-4, page 18] implies that $\tilde{v} \ge 0$.

Now, let $k = \max[(N\delta + \alpha)\theta/\gamma, \|\tilde{v}_0\|]$. Then $Lk + f(\sigma,\tau) \le 0$ and $\tilde{v}(\sigma,0) \le k$ for $\sigma \in [0,1]$. Therefore bound (34) follows by the parabolic comparison principle. □

Lemma 2. *Assume $\tilde{v}$ is continuous, bounded and nonnegative. Then if $T > 0$ is sufficiently small, there exist unique, continuous solutions $\tilde{x}$ and $\tilde{y}$ to the system (16)–(17), (23)–(24) on $[0,1]\times[0,T]$.*

Proof. Let $\xi(\tau)$ be as defined by system (31). Let $Z(\xi(\tau),\tau) = (\tilde{x}(\xi(\tau),\tau), \tilde{y}(\xi(\tau),\tau))^T$. Let $M > \max(\|\tilde{x}_0\|, \|\tilde{y}_0\|)$. We consider the complete metric space of functions $B_T \subset C[0,T]$ defined as

$$B_T = \{Z(\xi(\tau),\tau) \in C[0,T] : \|Z\| \le M \text{ and } Z(\xi(0),0) = Z_0(\xi(0))\}.$$

Note that B_T is nonempty since $Z(\xi(\tau),\tau) \equiv Z_0(\xi(0)) \in B_T$. Along the

characteristic curve $\xi(\tau)$ we can write the system (16)–(17) as

$$\frac{d}{d\tau}Z(\xi(\tau),\tau) = f(Z(\xi(\tau),\tau),\xi(\tau),\tau) + h(Z(\xi(\tau),\tau),\xi(\tau),\tau)\int_{I_{2r_c}(\xi(\tau),\tau)} Z(\omega,\tau)\,d\omega \quad (35)$$

where

$$f(Z,\xi(\tau),\tau) = \begin{bmatrix} \lambda+\mu-\rho\theta-\dfrac{\beta}{|I_{r_c}(\xi(\tau),\tau)|}\displaystyle\int_{I_{r_c}(\xi(\tau),\tau)}\tilde{v}\,d\omega & 0 \\ \dfrac{\beta}{|I_{r_c}(\xi(\tau),\tau)|}\displaystyle\int_{I_{r_c}(\xi(\tau),\tau)}\tilde{v}\,d\omega & \mu-\rho\theta-\delta \end{bmatrix} Z + Z\begin{bmatrix} -\dfrac{\lambda+\mu}{\theta} \\ -\dfrac{\mu-\delta}{\theta} \end{bmatrix}^T Z$$

and

$$h(Z,\xi(\tau),\tau) = \begin{bmatrix} \dfrac{\rho}{|I_{2r_c}(\xi(\tau),\tau)|} & 0 \\ 0 & 0 \end{bmatrix} Z.$$

Then, recalling the bounds for $|I_{r_c}(\xi(\tau),\tau)|$ given by inequality (33) and the fact that $\tilde{v}$ is bounded, it follows that f and h are Lipschitz continuous in Z and bounded on $B_T\times[0,1]\times[0,T]$. So there exist positive constants L_1 and L_2 such that, for any $Z_1, Z_2 \in B_T$, $\tau\in[0,T]$, $\xi(\tau)\in[0,1]$,

$$|f(Z_1(\xi(\tau),\tau),\xi(\tau),\tau) - f(Z_2(\xi(\tau),\tau),\xi(\tau),\tau)| \le L_1\|Z_1-Z_2\|,$$
$$|h(Z_1(\xi(\tau),\tau),\xi(\tau),\tau) - h(Z_2(\xi(\tau),\tau),\xi(\tau),\tau)| \le L_2\|Z_1-Z_2\|.$$

We define the mapping $\Phi: B_T\to C[0,T]$ by

$$\Phi(Z)(\xi(\tau),\tau) = Z_0(\xi(0)) + \int_0^\tau \left(f(Z(\xi(s),s),\xi(s),s) + h(Z(\xi(s),s),\xi(s),s)\int_{I_{2r_c}(\xi(s),s)} Z(\omega,s)\,d\omega\right) ds. \quad (36)$$

and observe that a solution to Eq. (35) must satisfy $\Phi(Z)=Z$. We claim that $\Phi: B_T\to B_T$. Indeed, let $Z(\xi(\tau),\tau)\in B_T$. Clearly $\Phi(Z)(\xi(\tau),\tau)\in C[0,1]$. It is also immediate that $\Phi(Z)(\xi(0),0)=Z_0(\xi(0))$. From Eq. (36) we see that, because M was chosen so that $\|Z_0\|<M$,

$$\|\Phi(Z)\| \le \|Z_0\| + \int_0^\tau \left(\|f\| + \|h\|\int_0^1 \|Z\|\,d\omega\right) ds \le \|Z_0\| + (\|f\| + M\|h\|)T \le M$$

for T sufficiently small. Therefore $\Phi(Z)(\xi(\tau),\tau)\in B_T$ and the claim holds.

Now we will prove that Φ is a contraction on B_T. Let $Z_1, Z_2\in B_T$. It follows from Eq. (36) that for any $\tau\in[0,T]$ and $\xi(\tau)\in[0,1]$,

$$\begin{aligned}
&|\Phi(Z_1)(\xi(\tau),\tau) - \Phi(Z_2)(\xi(\tau),\tau)| \\
&= \left|\int_0^\tau \left(f(Z_1(\xi(s),s),\xi(s),s) - f(Z_2(\xi(s),s),\xi(s),s) \right.\right. \\
&\quad + h(Z_1(\xi(s),s),\xi(s),s)\int_{I_{2r_c}(\xi(s),s)} Z_1(\omega,s)\,d\omega \\
&\quad \left.\left. - h(Z_2(\xi(s),s),\xi(s),s)\int_{I_{2r_c}(\xi(s),s)} Z_2(\omega,s)\,d\omega\right) ds\right| \\
&\le \int_0^\tau |f(Z_1(\xi(s),s),\xi(s),s) - f(Z_2(\xi(s),s),\xi(s),s)|\,ds \\
&\quad + \int_0^\tau \left| h(Z_1(\xi(s),s),\xi(s),s)\int_{I_{2r_c}(\xi(s),s)} Z_1(\omega,s)\,d\omega \right. \\
&\quad \left. - h(Z_1(\xi(s),s),\xi(s),s)\int_{I_{2r_c}(\xi(s),s)} Z_2(\omega,s)\,d\omega\right| ds \\
&\quad + \int_0^\tau \left| h(Z_1(\xi(s),s),\xi(s),s)\int_{I_{2r_c}(\xi(s),s)} Z_2(\omega,s)\,d\omega \right. \\
&\quad \left. - h(Z_2(\xi(s),s),\xi(s),s)\int_{I_{2r_c}(\xi(s),s)} Z_2(\omega,s)\,d\omega\right| ds \\
&\le \int_0^\tau |f(Z_1(\xi(s),s),\xi(s),s) - f(Z_2(\xi(s),s),\xi(s),s)|\,ds \\
&\quad + \int_0^\tau |h(Z_1(\xi(s),s),\xi(s),s)| \\
&\quad \times \left(\int_{I_{2r_c}(\xi(s),s)} |Z_1(\omega,s) - Z_2(\omega,s)|\,d\omega\right) ds \\
&\quad + \int_0^\tau |h(Z_1(\xi(s),s),\xi(s),s) \\
&\quad - h(Z_2(\xi(s),s),\xi(s),s)| \left(\int_{I_{2r_c}(\xi(s),s)} |Z_2(\omega,s)|\,d\omega\right) ds \\
&\le \int_0^\tau \left(L_1\|Z_1-Z_2\| + \|h\|\left(\int_0^1 \|Z_1-Z_2\|\,d\omega\right)\right. \\
&\quad \left. + L_2\|Z_1-Z_2\|\left(\int_0^1 M\,d\omega\right)\right) ds \\
&\le (L_1 + \|h\| + L_2M)T\cdot\|Z_1-Z_2\|.
\end{aligned}$$

Therefore, if T is sufficiently small,

$$\|\Phi(Z_1) - \Phi(Z_2)\| \le K\|Z_1-Z_2\|$$

for some $K\in[0,1)$. That is, Φ is a contraction on B_T for sufficiently small T. By the Contraction Mapping Theorem there exists a unique fixed point of Φ in B_T which is a solution to Eq. (35). □

3.3. Existence and uniqueness for the hyperbolic–parabolic subsystem

Given a fixed $\tilde{u}\in E_T$ we are now able to prove the existence and uniqueness of a solution to the coupled hyperbolic–parabolic system (16)–(18), (21)–(24) by considering a contraction on the space S_T defined in Section 3.1.

Theorem 1. *If $T>0$ is sufficiently small, then for any $\tilde{u}\in E_T$ there exists a unique, continuous solution $(\tilde{x},\tilde{y},\tilde{v})$ of the system (16)–(18), (21)–(24) on $[0,1]\times[0,T]$. Furthermore, for any $(\sigma,\tau)\in[0,1]\times[0,T]$,*

$$0\le\tilde{x}(\sigma,\tau)\le\theta, \qquad 0\le\tilde{y}(\sigma,\tau)\le\theta,$$
$$0\le\tilde{v}(\sigma,\tau)\le\max[(N\delta+\alpha)\theta/\gamma, \|\tilde{v}_0\|].$$

Proof. Let $\tilde{u}(\sigma,\tau)\in E_T$. Define $R(\tau)$ by Eq. (28). Observe that for any $(\sigma,\tau)\in[0,1]\times[0,T]$, $(\tilde{x}(\xi(\tau),\tau),\tilde{y}(\xi(\tau),\tau))\equiv(\tilde{x}_0(\sigma_0),\tilde{y}_0(\sigma_0))\in S_T$ where $\xi(0;\sigma,\tau)=\sigma_0$. Therefore S_T is nonempty. For $\hat{Z}=(\hat{x},\hat{y})\in S_T$, define a map $\mathcal{H}$ by the following. Given $\hat{Z}=(\hat{x},\hat{y})\in S_T$ first apply Lemma 1 to solve for $\tilde{v}$. Then given $\tilde{v}$, solve for $\tilde{x}$ and $\tilde{y}$ by Lemma 2. Let $\mathcal{H}(\hat{Z})=Z$ where $Z=(\tilde{x},\tilde{y})^T$.

Now we show that $\mathcal{H}: S_T\to S_T$. Let $(\hat{x},\hat{y})\in S_T$ and $\tilde{v}$ be the corresponding solution from Lemma 1.

From Eq. (16) it is clear that, along the characteristic curve $\xi(\tau)$,

$$\frac{d}{d\tau}(\tilde{x}(\xi(\tau),\tau)) = A_1(\tau,\xi(\tau),\hat{x},\hat{y})\tilde{x}(\xi(\tau),\tau)$$

for an appropriately chosen bounded function A_1. Therefore $\tilde{x}_0\ge 0$ implies that $\tilde{x}(\xi(\tau),\tau)\ge 0$. Recalling that $\tilde{v}\ge 0$ it follows then from Eq. (17) that

$$\frac{d}{d\tau}(\tilde{y}(\xi(\tau),\tau)) \ge A_2(\hat{x},\hat{y})\tilde{y}(\xi(\tau),\tau)$$

for an appropriately chosen bounded function A_2. Therefore $\tilde{y}_0 \geq 0$ implies that $\tilde{y}(\xi(\tau),\tau) \geq 0$. Let $\tilde{z} = \theta - \tilde{x} - \tilde{y}$. Then

$$\frac{d}{d\tau}(\tilde{z}(\xi(\tau),\tau)) = \frac{\rho\tilde{x}}{|I_{2r_c}(\xi(\tau),\tau)|}\int_{I_{2r_c}(\xi(\tau),\tau)} \theta - \tilde{x}\,d\omega + \rho\theta\tilde{y} - \mu\tilde{z} - \frac{\tilde{z}}{\theta}(\lambda\tilde{x} - \delta\tilde{y} - \mu\tilde{z}).$$

If $\tilde{x} + \tilde{y} = \theta$ then

$$\frac{d}{d\tau}(\tilde{z}(\xi(\tau),\tau)) \geq 0$$

implying $\tilde{x} + \tilde{y} \leq \theta$ for all τ. Therefore $(\tilde{x},\tilde{y}) \in S_T$.

It remains to show that $\mathcal{H}$ is a contraction for sufficiently small T. Let $\hat{Z}_1, \hat{Z}_2 \in S_T$ and $Z_i = \mathcal{H}\hat{Z}_i$ for $i = 1, 2$. Let v_i be the solution from Lemma 1 corresponding to Z_i. We first claim that there exists $C_0 > 0$ such that

$$\|\tilde{v}_1 - \tilde{v}_2\| \leq C_0\|\hat{Z}_1 - \hat{Z}_2\|. \tag{37}$$

Indeed, for L defined as in Lemma 1 we have $L(\tilde{v}_1 - \tilde{v}_2) + \tilde{f}(\sigma,\tau) = 0$ where

$$\tilde{f}(\sigma,\tau) = \frac{N\delta}{|I_{r_c}(\sigma,\tau)|}\int_{I_{r_c}(\sigma,\tau)}\left[r_c^2 - R^2(\tau)(\sigma-\omega)^2\right](\hat{y}_1 - \hat{y}_2)\,d\omega - \frac{\alpha}{|I_{r_c}(\sigma,\tau)|}\int_{I_{r_c}(\sigma,\tau)}(\hat{x}_1 - \hat{x}_2)\,d\omega.$$

Let $k = N\delta\|\hat{y}_1 - \hat{y}_2\|/\gamma + \alpha\|\hat{x}_1 - \hat{x}_2\|/\gamma$. Then $Lk + \tilde{f}(\sigma,\tau) \leq 0$ and $(\tilde{v}_1 - \tilde{v}_2)(\sigma,0) = 0$ for $\sigma \in [0,1]$. Therefore the parabolic comparison principle [23, Theorem 1.2-4, page 18] implies that for all $(\sigma,\tau) \in [0,1]\times[0,T]$, $|(\tilde{v}_1 - \tilde{v}_2)(\sigma,\tau)| \leq k$ and thus we derive inequality (37).

By formally integrating Eqs. (16) and (17) along the characteristic, we see that for $i = 1, 2$, Z_i must satisfy

$$Z_i(\xi(\tau),\tau) = Z_0(\xi(0)) + \int_0^\tau \Big[f(Z_i(\xi(s),s)) + g(Z_i(\xi(s),s),\xi(s),s)\int_{I_{r_c}(\xi(s),s)}\tilde{v}_i(\omega,s)\,d\omega + h(Z_i(\xi(s),s),\xi(s),s)\int_{I_{2r_c}(\xi(s),s)} Z_i(\omega,s)\,d\omega\Big]\,ds \tag{38}$$

with

$$f(Z) = \begin{bmatrix}\lambda+\mu-\rho\theta & 0\\ 0 & \mu-\rho\theta-\delta\end{bmatrix}Z + Z\begin{bmatrix}-\frac{\lambda+\mu}{\theta}\\ -\frac{\mu-\delta}{\theta}\end{bmatrix}^T Z,$$

$$g(Z,\xi(s),s) = \begin{bmatrix}-\frac{\beta}{|I_{r_c}(\xi(s),s)|} & 0\\ \frac{\beta}{|I_{r_c}(\xi(s),s)|} & 0\end{bmatrix}Z \quad \text{and}$$

$$h(Z,\xi(s),s) = \begin{bmatrix}\frac{\rho}{|I_{2r_c}(\xi(s),s)|} & 0\\ 0 & 0\end{bmatrix}Z.$$

It follows that f, g, and h are Lipschitz continuous in Z and bounded on B_T, $B_T\times[0,1]\times[0,T]$ and $B_T\times[0,1]\times[0,T]$, respectively. Therefore there exist positive C_1, C_2, and C_3 such that for any $Z_1, Z_2 \in B_T$, $\tau \in [0,T]$, and $\xi(\tau) \in [0,1]$,

$$|f(Z_1(\xi(\tau),\tau)) - f(Z_2(\xi(\tau),\tau))| \leq C_1\|Z_1 - Z_2\|,$$
$$|g(Z_1(\xi(\tau),\tau),\xi(\tau),\tau) - g(Z_2(\xi(\tau),\tau),\xi(\tau),\tau)| \leq C_2\|Z_1 - Z_2\|,$$
$$|h(Z_1(\xi(\tau),\tau),\xi(\tau),\tau) - h(Z_2(\xi(\tau),\tau),\xi(\tau),\tau)| \leq C_3\|Z_1 - Z_2\|.$$

From Eq. (38) we can then determine that for any $\tau \in [0,T]$,

$$\begin{aligned}
&|Z_1(\xi(\tau),\tau) - Z_2(\xi(\tau),\tau)|\\
&= \Big|\int_0^\tau \Big(f(Z_1) - f(Z_2) + g(Z_1,\xi(s),s)\int_{I_{r_c}(\xi(s),s)}\tilde{v}_1\,d\omega\\
&\quad - g(Z_2,\xi(s),s)\int_{I_{r_c}(\xi(s),s)}\tilde{v}_2\,d\omega\\
&\quad + h(Z_1,\xi(s),s)\int_{I_{2r_c}(\xi(s),s)} Z_1\,d\omega\\
&\quad - h(Z_2,\xi(s),s)\int_{I_{2r_c}(\xi(s),s)} Z_2\,d\omega\Big)\,ds\Big|\\
&= \Big|\int_0^\tau \Big(f(Z_1) - f(Z_2) + g(Z_1,\xi(s),s)\int_{I_{r_c}(\xi(s),s)}(\tilde{v}_1 - \tilde{v}_2)\,d\omega\\
&\quad + (g(Z_1,\xi(s),s) - g(Z_2,\xi(s),s))\int_{I_{r_c}(\xi(s),s)}\tilde{v}_2\,d\omega\\
&\quad + h(Z_1,\xi(s),s)\int_{I_{2r_c}(\xi(s),s)}(Z_1 - Z_2)\,d\omega\\
&\quad + (h(Z_1,\xi(s),s) - h(Z_2,\xi(s),s))\int_{I_{2r_c}(\xi(s),s)} Z_2\,d\omega\Big)\,ds\Big|\\
&\leq \int_0^\tau \Big(|f(Z_1) - f(Z_2)| + |g(Z_1,\xi(s),s)|\int_0^1 |\tilde{v}_1 - \tilde{v}_2|\,d\omega\\
&\quad + |g(Z_1,\xi(s),s) - g(Z_2,\xi(s),s)|\int_0^1 |\tilde{v}_2|\,d\omega\\
&\quad + |h(Z_1,\xi(s),s)|\int_0^1 |Z_1 - Z_2|\,d\omega + |h(Z_1,\xi(s),s)\\
&\quad - h(Z_2,\xi(s),s)|\int_0^1 |Z_2|\,d\omega\Big)\,ds\\
&\leq \int_0^\tau \big(C_1\|Z_1 - Z_2\| + \|g\|\cdot\|\tilde{v}_1 - \tilde{v}_2\| + C_2\|\tilde{v}_2\|\cdot\|Z_1 - Z_2\|\\
&\quad + \|h\|\cdot\|Z_1 - Z_2\| + C_3\|Z_2\|\cdot\|Z_1 - Z_2\|\big)\,ds.
\end{aligned}$$

It follows from inequality (34) that

$$\|Z_1 - Z_2\| \leq \|g\|\cdot\|\tilde{v}_1 - \tilde{v}_2\|T + \int_0^\tau C_4\|Z_1 - Z_2\|\,ds$$

for some $C_4 > 0$. Therefore by Gronwall's inequality and inequality (37),

$$\begin{aligned}
\|Z_1 - Z_2\| &\leq \|g\|\cdot\|\tilde{v}_1 - \tilde{v}_2\|T\exp\left(\int_0^\tau C_4\,ds\right)\\
&\leq \|g\|\cdot\|\tilde{v}_1 - \tilde{v}_2\|T\exp(C_4T)\\
&\leq \|g\|\exp(C_4T)TC_0\|\hat{Z}_1 - \hat{Z}_2\|.
\end{aligned}$$

Therefore $\mathcal{H}$ is a contraction for T sufficiently small since $\|g\|\exp(C_4T)TC_0 \to 0$ as $T \to 0$. By the Contraction Mapping Theorem there exists a unique fixed point $(\tilde{x},\tilde{y})$ of $\mathcal{H}$ in S_T and a corresponding $\tilde{v}$ such that $(\tilde{x},\tilde{y},\tilde{v})$ is a solution to the system (16)–(18), (21)–(24). □

3.4. Existence and uniqueness for the full system

Theorem 1 provides a map from $\tilde{u} \in E_T$ to a solution $(\tilde{x},\tilde{y},\tilde{v})$ of the hyperbolic–parabolic subsystem. Thus, by considering a contraction on E_T, we are ready to prove in Theorem 2 the main result of this section, existence and uniqueness of local solutions to the full system (16)–(26). Lemma 3 then extends the local solutions to global solutions.

Theorem 2. *If $T > 0$ is sufficiently small, then there exists a unique, continuous solution $(\tilde{x},\tilde{y},\tilde{v},\tilde{u},R)$ to the system (16)–(26) on $[0,1]\times[0,T]$.*

Proof. For $\tilde{u} \in E_T$, we define a map $\mathcal{F} : \tilde{u}(\sigma,\tau) \to \tilde{w}(\sigma,\tau)$ by first solving for $(\tilde{x},\tilde{y},\tilde{v})$ by Theorem 1. Then we define

$$\tilde{w}(\sigma,\tau) = \frac{R(\tau)}{\theta\sigma^2}\int_0^\sigma \omega^2[-\mu\theta + (\lambda+\mu)\tilde{x}(\omega,\tau) + (\mu-\delta)\tilde{y}(\omega,\tau)]\,d\omega, \quad \tilde{w}(0,\tau) = 0. \tag{39}$$

We claim that $\mathcal{F} : E_T \to E_T$. Let $\tilde{u} \in E_T$ and $\tilde{w} = \mathcal{F}\tilde{u}$. Then clearly $\tilde{w}(\sigma,\tau) \in C([0,1]\times[0,T])$ since $\tilde{x}, \tilde{y}$, and $R(\tau)$ are continuous and $\tilde{w}(\sigma,0) = \tilde{u}_0(\sigma)$. Furthermore,

$$-(\mu+\delta)\theta \le -\mu\theta + (\lambda+\mu)\tilde{x}(\omega,\tau) + (\mu-\delta)\tilde{y}(\omega,\tau) \le \lambda\theta$$

implies that

$$-\frac{(\mu+\delta)}{3}R(\tau) \le \tilde{w}(\sigma,\tau) \le \frac{\lambda}{3}R(\tau).$$

By inequality (29) we conclude that

$$\|\tilde{w}\| \le \max\left(\frac{\mu+\delta}{3}, \frac{\lambda}{3}\right)(R_0 + LT) < L + \max\left(\frac{\mu+\delta}{3}, \frac{\lambda}{3}\right)LT.$$

So for T sufficiently small, $\|\tilde{w}\| \le L$. Finally let $\sigma_1, \sigma_2 \in [0,1]$ and $\tau \in [0,T]$. Without loss of generality, assume $\sigma_2 < \sigma_1$. Then,

$$\begin{aligned}
&|\tilde{w}(\sigma_1,\tau) - \tilde{w}(\sigma_2,\tau)| \\
&= \left|\frac{R(\tau)}{\theta\sigma_1^2}\int_0^{\sigma_1} \omega^2\left[-\mu\theta + (\lambda+\mu)\tilde{x}(\omega,\tau) + (\mu-\delta)\tilde{y}(\omega,\tau)\right]d\omega \right. \\
&\quad \left. - \frac{R(\tau)}{\theta\sigma_2^2}\int_0^{\sigma_2} \omega^2\left[-\mu\theta + (\lambda+\mu)\tilde{x}(\omega,\tau) + (\mu-\delta)\tilde{y}(\omega,\tau)\right]d\omega\right| \\
&= \frac{R(\tau)}{\theta}\left|\left(\frac{1}{\sigma_1^2} - \frac{1}{\sigma_2^2}\right)\int_0^{\sigma_2} \omega^2[-\mu\theta + (\lambda+\mu)\tilde{x}(\omega,\tau) \right. \\
&\quad + (\mu-\delta)\tilde{y}(\omega,\tau)]\,d\omega \\
&\quad \left. + \frac{1}{\sigma_1^2}\int_{\sigma_2}^{\sigma_1} \omega^2[-\mu\theta + (\lambda+\mu)\tilde{x}(\omega,\tau) + (\mu-\delta)\tilde{y}(\omega,\tau)]\,d\omega\right| \\
&\le \frac{R(\tau)}{\theta}\left[\frac{(\sigma_1+\sigma_2)(\sigma_1-\sigma_2)\sigma_2\max(\mu+\delta,\lambda)\theta}{3\sigma_1^2} \right. \\
&\quad \left. + \frac{\max(\mu+\delta,\lambda)\theta\,(\sigma_1^3 - \sigma_2^3)}{3\sigma_1^2}\right] \\
&\le R(\tau)\max\left(\frac{\mu+\delta}{3}, \frac{\lambda}{3}\right)(\sigma_1-\sigma_2)\left[\frac{2\sigma_2}{\sigma_1} + \frac{\sigma_1^2+\sigma_1\sigma_2+\sigma_2^2}{\sigma_1^2}\right] \\
&< 5R(\tau)\max\left(\frac{\mu+\delta}{3}, \frac{\lambda}{3}\right)(\sigma_1-\sigma_2) \\
&< 5(R_0+TL)\frac{L}{R_0}(\sigma_1-\sigma_2) \\
&\le K(\sigma_1-\sigma_2).
\end{aligned}$$

Hence $\tilde{w} \in E_T$.

To show that $\mathcal{F}$ is a contraction, let $w_i = \mathcal{F}u_i$ and

$$R_i(\tau) = R_0 + \int_0^\tau u_i(1,s)\,ds \tag{40}$$

for $i = 1, 2$. Let C_i throughout be an appropriately chosen positive constant. For any $\sigma \in (0,1]$ and $\tau \in [0,T]$, it follows from Eq. (39) that

$$\begin{aligned}
&|w_1(\sigma,\tau) - w_2(\sigma,\tau)| \\
&= \left|\frac{R_1(\tau)}{\theta\sigma^2}\int_0^\sigma \omega^2[-\mu\theta + (\lambda+\mu)\tilde{x}_1(\omega,\tau) + (\mu-\delta)\tilde{y}_1(\omega,\tau)]\,d\omega \right. \\
&\quad - \frac{R_2(\tau)}{\theta\sigma^2}\int_0^\sigma \omega^2[-\mu\theta + (\lambda+\mu)\tilde{x}_2(\omega,\tau) \\
&\quad \left. + (\mu-\delta)\tilde{y}_2(\omega,\tau)]\,d\omega\right| \\
&\le \left|\frac{(R_1(\tau)-R_2(\tau))}{\theta\sigma^2}\int_0^\sigma \omega^2[-\mu\theta + (\lambda+\mu)\tilde{x}_1(\omega,\tau) \right. \\
&\quad \left. + (\mu-\delta)\tilde{y}_1(\omega,\tau)]\,d\omega\right| + \left|\frac{R_2(\tau)}{\theta\sigma^2}\int_0^\sigma \omega^2 \right. \\
&\quad \times [(\lambda+\mu)(\tilde{x}_1(\omega,\tau) - \tilde{x}_2(\omega,\tau)) \\
&\quad \left. + (\mu-\delta)(\tilde{y}_1(\omega,\tau) - \tilde{y}_2(\omega,\tau))]\,d\omega\right| \\
&:= I_1 + I_2.
\end{aligned}$$

By Eq. (40) we have

$$\begin{aligned}
|I_1| &\le \frac{|R_1(\tau)-R_2(\tau)|}{\theta\sigma^2}\int_0^\sigma \omega^2|-\mu\theta + (\lambda+\mu)\tilde{x}_1(\omega,\tau) \\
&\quad + (\mu-\delta)\tilde{y}_1(\omega,\tau)|\,d\omega \\
&= \frac{\left|\int_0^\tau u_1(1,s) - u_2(1,s)\,ds\right|}{\theta\sigma^2}\int_0^\sigma \omega^2|-\mu\theta + (\lambda+\mu)\tilde{x}_1(\omega,\tau) \\
&\quad + (\mu-\delta)\tilde{y}_1(\omega,\tau)|\,d\omega \\
&\le \frac{T\|u_1-u_2\|}{\theta\sigma^2}\int_0^\sigma \omega^2\left(\mu\theta + (\lambda+\mu)\|\tilde{x}_1\| + |\mu-\delta|\cdot\|\tilde{y}_1\|\right)d\omega \\
&\le \frac{TC_1\sigma}{3\theta}\|u_1-u_2\| \\
&\le C_2T\|u_1-u_2\|.
\end{aligned}$$

To estimate I_2 we will first consider $\|Z_1 - Z_2\|$ with $Z_i = (\tilde{x}_i, \tilde{y}_i)^T$ and satisfying Eq. (35) as in Lemma 2. For $(\sigma,\tau) \in [0,1]\times[0,T]$ and for $i = 1, 2$, let $\xi_i(s) = \xi_i(s;\sigma,\tau)$ be the backwards characteristic curve for Z_i through the point (σ,τ). Let $\epsilon = \frac{2r_c}{R(\tau)}$. It follows that

$$\begin{aligned}
Z_1(\sigma,\tau) - Z_2(\sigma,\tau) &= Z_0(\xi_1(0)) - Z_0(\xi_2(0)) \\
&\quad + \int_0^\tau [f(Z_1(\xi_1(s)),\xi_1(s),s) \\
&\quad - f(Z_2(\xi_2(s)),\xi_2(s),s)]\,ds \\
&\quad + \int_0^\tau \left[h(Z_1(\xi_1(s)),\xi_1(s),s)\int_{l_{2r_c}(\xi_1(s),s)} Z_1\,d\omega \right. \\
&\quad \left. - h(Z_2(\xi_2(s)),\xi_2,s)\int_{l_{2r_c}(\xi_2(s),s)} Z_2\,ds\omega\right]ds \\
&:= J_1 + J_2 + J_3.
\end{aligned}$$

To estimate J_i we need to estimate $|\xi_1(s;\sigma,\tau) - \xi_2(s;\sigma,\tau)|$. From system (31) we have

$$\begin{aligned}
\frac{d(\xi_1(s)-\xi_2(s))}{ds} &= \left(-\frac{\xi_1(s)}{R_1(s)}\frac{dR_1(s)}{ds} + \frac{\tilde{u}_1(\xi_1(s),s)}{R_1(s)}\right) \\
&\quad - \left(-\frac{\xi_2(s)}{R_2(s)}\frac{dR_2(s)}{ds} + \frac{\tilde{u}_2(\xi_2(s),s)}{R_2(s)}\right) \\
&= -\frac{1}{R_1(s)}\frac{dR_1(s)}{ds}(\xi_1(s)-\xi_2(s)) \\
&\quad - \xi_2(s)\left(\frac{1}{R_1(s)}\frac{dR_1(s)}{ds} - \frac{1}{R_2(s)}\frac{dR_2(s)}{ds}\right) \\
&\quad + \frac{\tilde{u}_1(\xi_1(s),s)}{R_1(s)R_2(s)}(R_2(s)-R_1(s)) \\
&\quad + \frac{1}{R_2(s)}(\tilde{u}_1(\xi_1(s),s) - \tilde{u}_1(\xi_2(s),s)) \\
&\quad + \frac{1}{R_2(s)}(\tilde{u}_1(\xi_2(s),s) - \tilde{u}_2(\xi_2(s),s)).
\end{aligned}$$

Recalling inequalities (29) and (30) we observe that each term on the right hand side is bounded by a constant multiple of either $\|\tilde{u}_1 - \tilde{u}_2\|$

or $\|\xi_1 - \xi_2\|$. Therefore, by integrating, we have for $0 \le s \le \tau$

$$|\xi_1(s;\sigma,\tau) - \xi_2(s;\sigma,\tau)| \le \int_s^\tau C_3\|\tilde{u}_1 - \tilde{u}_2\| + C_4\|\xi_1 - \xi_2\|dt$$

and therefore

$$\|\xi_1 - \xi_2\| \le C_3T\|\tilde{u}_1 - \tilde{u}_2\| + \int_0^\tau C_4\|\xi_1 - \xi_2\|dt.$$

Then Gronwall's inequality implies

$$\|\xi_1 - \xi_2\| \le C_5T\|\tilde{u}_1 - \tilde{u}_2\|. \tag{41}$$

$Z_0(\sigma)$ is Lipschitz continuous since it is continuously differentiable on $[0, 1]$. Therefore,

$$|J_1| \le C_6\|\xi_1 - \xi_2\|. \tag{42}$$

We now define the function

$$j(g, \xi(s), s) := \int_{I_{2r_c}(\xi(s),s)} g\, d\omega$$

for $s \in [0, T]$, $\xi(s) \in [0, 1]$ and $g \in L^\infty([0, 1])$. Note that $j(g, \xi(s), s)$ is clearly Lipschitz continuous in g. Additionally, we claim that j is Lipschitz continuous in ξ. Indeed,

$$\begin{aligned}
&|j(g, \xi_1(s), s) - j(g, \xi_2(s), s)| \\
&= \left|\int_{I_{2r_c}(\xi_1(s),s)} g\, d\omega - \int_{I_{2r_c}(\xi_2(s),s)} g\, d\omega\right| \\
&\le \left|\int_{I_{2r_c}(\xi_1(s),s)} g\, d\omega - \int_{I_{2r_c}(\xi_1(s),s)\cap I_{2r_c}(\xi_2(s),s)} g\, d\omega\right| \\
&\quad + \left|\int_{I_{2r_c}(\xi_1(s),s)\cap I_{2r_c}(\xi_2(s),s)} g\, d\omega - \int_{I_{2r_c}(\xi_2(s),s)} g\, d\omega\right| \\
&= \left|\int_{I_{2r_c}(\xi_1(s),s)\setminus I_{2r_c}(\xi_2(s),s)} g\, d\omega\right| \\
&\quad + \left|\int_{I_{2r_c}(\xi_2(s),s)\setminus I_{2r_c}(\xi_1(s),s)} g\, d\omega\right|
\end{aligned}$$

If $I_{2r_c}(\xi_1(s), s)$ and $I_{2r_c}(\xi_2(s), s)$ are disjoint, then $|I_{2r_c}(\xi_i(s), s)| \le \frac{2r_c}{R(\tau)} \le |\xi_2(s) - \xi_1(s)|$ for $i = 1, 2$. If $I_{2r_c}(\xi_1(s), s) \cap I_{2r_c}(\xi_2(s), s) \ne \emptyset$, then necessarily $|I_{2r_c}(\xi_1(s), s) \setminus I_{2r_c}(\xi_2(s), s)| < |\xi_2(s) - \xi_1(s)|$ and likewise for $|I_{2r_c}(\xi_2(s), s) \setminus I_{2r_c}(\xi_1(s), s)|$. In either case, it follows from above that

$$|j(g, \xi_1(s), s) - j(g, \xi_2(s), s)| \le 2\|g\|_\infty \cdot |\xi_2(s) - \xi_1(s)|.$$

Hence f and $j(\xi(s), s, Z)$ are Lipschitz continuous in ξ. We also have that, for any ξ and Z, $|j(Z, \xi(s), s)| \le M$. We recall from Lemma 2 that f is Lipschitz continuous in Z and bounded.

Let $L_1, L_2, ..., L_5$ be positive constants such that for any $Z, Z_1, Z_2, \xi, \xi_1, \xi_2, s$,

$$\begin{aligned}
|f(Z, \xi_1(s), s) - f(Z, \xi_2(s), s)| &\le L_1|\xi_1(s) - \xi_2(s)|, \\
|f(Z_1, \xi(s), s) - f(Z_2, \xi(s), s)| &\le L_2|Z_1 - Z_2|, \\
|h(Z_1, \xi_1(s), s) - h(Z_2, \xi_2(s), s)| &\le L_3|Z_1 - Z_2|, \\
|j(Z, \xi_1(s), s) - j(Z, \xi_2(s), s)| &\le L_4|\xi_1(s) - \xi_2(s)|, \\
|j(Z_1, \xi(s), s) - j(Z_2, \xi(s), s)| &\le L_5|Z_1 - Z_2|.
\end{aligned}$$

The existence of L_3 follows from inequality (33) which proves that $|I_{2r_c}(\xi(s), s)|$ is bounded independent of ξ. We also recall that h is bounded.

Now to estimate $|J_2|$ we calculate that

$$\begin{aligned}
&|f(Z_1(\xi_1(s), s), \xi_1(s), s) - f(Z_2(\xi_2(s), s), \xi_2(s), s)| \\
&\le |f(Z_1(\xi_1(s), s), \xi_1(s), s) - f(Z_1(\xi_1(s), s), \xi_2(s), s)| \\
&\quad + |f(Z_1(\xi_1(s), s), \xi_2(s), s) - f(Z_1(\xi_2(s), s), \xi_2(s), s)| \\
&\quad + |f(Z_1(\xi_2(s), s), \xi_2(s), s) - f(Z_2(\xi_2(s), s), \xi_2(s), s)| \\
&\le L_1|\xi_1(s) - \xi_2(s)| + L_2|Z_1(\xi_1(s), s) - Z_1(\xi_2(s), s)| \\
&\quad + L_2|Z_1(\xi_2(s), s) - Z_2(\xi_2(s), s)| \\
&\le L_1|\xi_1(s) - \xi_2(s)| + L_2L_5|\xi_1(s) - \xi_2(s)| + L_2\|Z_1 - Z_2\|
\end{aligned}$$

from which it follows that

$$|J_2| \le C_7T\|\xi_1 - \xi_2\| + \int_0^\tau L_2\|Z_1 - Z_2\|\, ds. \tag{43}$$

To estimate $|J_3|$ we must first consider that by Eq. (35) we have, for any ξ_1 and ξ_2,

$$\begin{aligned}
&|Z(\xi_1(\tau), \tau) - Z(\xi_2(\tau), \tau)| = Z_0(\xi_1(0)) - Z_0(\xi_2(0)) \\
&\quad + \int_0^\tau [f(Z(\xi_1(s), s), \xi_1(s), s) - f(Z(\xi_2(s), s), \xi_2(s), s)]\, ds \\
&\quad + \int_0^\tau [h(Z(\xi_1(s), s), \xi_1(s), s)j(Z, \xi_1(s), s) \\
&\quad - h(Z_2(\xi_2(s), s), \xi_2(s), s)j(Z, \xi_2(s), s)]\, ds \\
&\le C_6\|\xi_1 - \xi_2\| + \int_0^\tau |f(Z(\xi_1(s), s), \xi_1(s), s) \\
&\quad - f(Z(\xi_1(s), s), \xi_2(s), s)|\, ds + \int_0^\tau |f(Z(\xi_1(s), s), \xi_2(s), s) \\
&\quad - f(Z(\xi_2(s), s), \xi_2(s), s)|\, ds \\
&\quad + \int_0^\tau |h(Z(\xi_1(s), s), \xi_1(s), s)| \cdot |j(Z, \xi_1(s), s) - j(Z, \xi_2(s), s)|\, ds \\
&\quad + \int_0^\tau |j(Z, \xi_2(s), s)| \cdot |h(Z(\xi_1(s), s), \xi_1(s), s) \\
&\quad - h(Z(\xi_2(s), s), \xi_2(s), s)|\, ds \\
&\le C_6\|\xi_1 - \xi_2\| + \int_0^\tau L_1|\xi_2(s) - \xi_2(s)| \\
&\quad + L_2|Z(\xi_1(s), s) - Z(\xi_2(s), s)|\, ds + \int_0^\tau \|h\|L_4|\xi_1(s) - \xi_2(s)| \\
&\quad + ML_3|Z(\xi_1(s), s) - Z(\xi_2(s), s)|\, ds.
\end{aligned}$$

Therefore

$$\begin{aligned}
|Z(\xi_1(\tau), \tau) - Z(\xi_2(\tau), \tau)| &\le C_8\|\xi_1 - \xi_2\| \\
&\quad + \int_0^\tau C_9|Z(\xi_1(s), s) - Z(\xi_2(s), s)|\, ds
\end{aligned}$$

and Gronwall's inequality gives positive L_6 such that, for any Z and $\tau \in [0, 1]$,

$$|Z(\xi_1(\tau), \tau) - Z(\xi_2(\tau), \tau)| \le L_6\|\xi_1 - \xi_2\|. \tag{44}$$

Finally we can estimate $|J_3|$. It holds that

$$\begin{aligned}
&\Big|h(Z_1(\xi_1(s), s), \xi_1(s), s) \int_{I_{2r_c}(\xi_1(s),s)} \\
&\qquad \times Z_1\, d\omega - h(Z_2(\xi_2(s), s), \xi_2(s), s) \int_{I_{2r_c}(\xi_2(s),s)} Z_2\, d\omega\Big| \\
&= |h(Z_1(\xi_1(s), s), \xi_1(s), s)j(\xi_1(s), Z_1) \\
&\quad - h(Z_2(\xi_2(s), s), \xi_2(s), s)j(\xi_2(s), Z_2)| \\
&\le |h(Z_1(\xi_1(s), s), \xi_1(s), s)j(\xi_1(s), Z_1) \\
&\quad - h(Z_1(\xi_2(s), s), \xi_1(s), s)j(\xi_1(s), Z_1)| \\
&\quad + |h(Z_1(\xi_2(s), s), \xi_1(s), s)j(\xi_1(s), Z_1) \\
&\quad - h(Z_2(\xi_2(s), s), \xi_2(s), s)j(\xi_1(s), Z_1)| \\
&\quad + |h(Z_2(\xi_2(s), s), \xi_2(s), s)j(\xi_1(s), Z_1) \\
&\quad - h(Z_2(\xi_2(s), s), \xi_2(s), s)j(\xi_1(s), Z_2)| \\
&\quad + |h(Z_2(\xi_2(s), s), \xi_2(s), s)j(\xi_1(s), Z_2) \\
&\quad - h(Z_2(\xi_2(s), s), \xi_2(s), s)j(\xi_2(s), Z_2)| \\
&\le |j(\xi_1(s), Z_1)| \cdot |h(Z_1(\xi_1(s), s), \xi_1(s), s) \\
&\quad - h(Z_1(\xi_2(s), s), \xi_1(s), s)| \\
&\quad + |j(\xi_1(s), Z_1)| \cdot |h(Z_1(\xi_2(s), s), \xi_1(s), s)
\end{aligned}$$

Table 1
Model parameters as estimated for a fusogenic oncolytic herpes simplex virus.

Parameter	Description	Value [Reference]
λ	Proliferation rate of uninfected cells	0.48 day^{-1} [24]
β	Viral infection coefficient	1.7×10^{-8} mm^3 day^{-1} virus^{-1} [24]
ρ	Cell-to-cell fusion coefficient	0–1.5×10^{-6} mm^3 day^{-1} cell^{-1} [estimated]
δ	Lysis rate of infected cells	1.5 day^{-1} [26]
μ	Death rate of syncytia	0.5 day^{-1} [4]
γ	Clearance rate of free virus	0.6 day^{-1} [24]
N	Viral burst size	10–100 viruses cell^{-1} [24]
α	Viral budding coefficient	1.5 viruses cell^{-1} day^{-1} [estimated]
θ	Density of tumor cells	10^6 cells mm^{-3} [24]
κ	Diffusion coefficient of free virus	0.864 mm^2 day^{-1} [24]
r_c	Radius of a cell	0.005 mm [15]

$$
\begin{aligned}
&- h(Z_2(\xi_2(s),s),\xi_2(s),s)|\\
&+ |h(Z_2(\xi_2(s),s),\xi_2(s),s)|\cdot|j(\xi_1(s),Z_1)-j(\xi_1(s),Z_2)|\\
&+ |h(Z_2(\xi_2(s),s),\xi_2(s),s)|\cdot|j(\xi_1(s),Z_2)-j(\xi_2(s),Z_2)|\\
&\le ML_3|Z_1(\xi_1(s),s)-Z_1(\xi_2(s),s)|\\
&+ ML_3|Z_1(\xi_2(s),s)-Z_2(\xi_2(s),s)|\\
&+ L_5\|h\|\cdot\|Z_1-Z_2\|+L_4\|h\|\cdot\|\xi_1-\xi_2\|\\
&\le C_{10}\|\xi_1-\xi_2\|+C_{11}\|Z_1-Z_2\|
\end{aligned}
$$

where the last inequality holds by (44). Hence,

$$|J_3|\le C_{10}T\|\xi_1-\xi_2\|+\int_0^\tau C_{11}\|Z_1-Z_2\|\,ds. \tag{45}$$

By summing inequalities (42), (43), and (45), and recalling (41), we calculate that for T sufficiently small,

$$\|Z_1-Z_2\|\le C_{12}T\|\tilde u_1-\tilde u_2\|+\int_0^\tau C_{13}\|Z_1-Z_2\|\,ds$$

from which Gronwall's inequality implies that

$$\|Z_1-Z_2\|\le C_{12}T\exp(C_{13}T)\|\tilde u_1-\tilde u_2\|.$$

Finally we have,

$$|I_2|\le\frac{|R_2(\tau)|}{\theta\sigma^2}\int_0^\sigma\omega^2C_{14}T\|u_1-u_2\|\,d\omega\le C_{15}T\|u_2-u_2\|$$

and therefore

$$\|\tilde w_1-\tilde w_2\|\le C_{16}T\|\tilde u_1-\tilde u_2\|.$$

Thus $\mathcal{F}$ is a contraction for T sufficiently small. By the Contraction Mapping Theorem there exists a unique fixed point $\tilde u$ of $\mathcal{F}$ in E_T and corresponding $\tilde x,\tilde y,\tilde v,R$ which solve the system (16)–(26) on $[0,1]\times[0,T]$. □

Lemma 3. *Any local solution to (16)–(26) (whose existence is guaranteed by Theorem 2) can be uniquely extended to a global solution for all $t\ge0$.*

Proof. Suppose there is a local solution with a maximal interval of existence $[0,\tilde T]$ for some $\tilde T>0$. Then this solution can be extended as follows to $[0,\tilde T+\epsilon]$ for some $\epsilon>0$.

We observe that, in fact, $|\frac{dR}{d\tau}/R|$ is uniformly bounded. Indeed, by Eqs. (19) and (20),

$$\left|\frac1R\cdot\frac{dR}{d\tau}\right|\le\frac13\max(\mu+\delta,\lambda) \tag{46}$$

which implies that the tumor radius neither blows up nor shrinks to zero in finite time. We take $t_0=\tilde T-\eta$ for $\eta>0$ as the initial time. Our observation (46) implies that we can appropriately choose constants L and K as in (27) in the definition of $E_{\eta+\epsilon}$, and uniformly bound $|I_{r_c}(\xi(\tau),\tau)|$ as in inequality (33), independent of η. Thus for η arbitrarily small, we could extend the solution to $[0,\tilde T+\epsilon]$ by proceeding as in Lemmas 1 and 2 and Theorems 1 and 2. □

4. Numerical results

4.1. Parameter estimation

With the inclusion of lysis, fusion and budding, our model can be tailored to a range of oncolytic viruses with differing viral spread mechanisms. For the sake of the following numerical simulations, we will parameterize the model for an oncolytic herpes simplex virus of syncytial phenotype, such as that of Fu et al. [6].

We assume τ and σ to have units of day and millimeter (mm), respectively. We take the parameter values for $\lambda,\beta,\gamma,\theta$, and κ used by Friedman et al. [24] which were estimated from experimental data on oncolytic herpes simplex virus (HSV-1) for the treatment of gliomas [25]. The lytic cycle of HSV-1 is approximately 12–16 h [26]. Accordingly, we take δ, the lysis rate of infected tumor cells, to be 1.5 day^{-1}. A typical cell diameter is 10^{-2} mm [15]; we take $r_c=0.005$ mm. A syncytium may survive from 12 to 120 h [4]; we take $\mu=0.5$ day^{-1}. Viral budding was not observed in HSV-1 by Nii et al. [27]; therefore, we choose $\alpha=1.5$ viruses cell^{-1} day^{-1} to be almost negligible compared to lysis, corresponding to the release of only one virion over the average lifetime of an infected cell.

In the following simulations we will vary the values for ρ and N to demonstrate a range of dynamical behaviors. For oncolytic HSV-1 the viral burst size, N, ranges from 10 to 100 [24]. We choose theoretical values for ρ in the range of 0 to 1.5×10^{-6} mm^3 day^{-1} cell^{-1}. The parameter descriptions, values and references are summarized in Table 1. Nondimensionalized parameters are calculated appropriately from the values in Table 1 as described in Section 4.2.

4.2. Nondimensionalization

We nondimensionalized the model (16)–(26) by setting $\bar x=\tilde x/\theta$, $\bar y=\tilde y/\theta$, and $\bar v=\tilde v/\theta$. Correspondingly, the following parameters are nondimensionalized:

$$\bar\beta=\beta N\theta,\quad \bar\rho=\rho\theta,\quad\text{and}\quad\bar\alpha=\frac{\alpha}{N}.$$

Dropping the bar notation for simplicity, we obtain the following nondimensionalized model for $\sigma\in(0,1]$ and $\tau>0$:

$$
\begin{aligned}
&\frac{\partial x(\sigma,\tau)}{\partial\tau}+\left[-\frac{\sigma}{R(\tau)}\frac{dR(\tau)}{d\tau}+\frac{u(\sigma,\tau)}{R(\tau)}\right]\frac{\partial x(\sigma,\tau)}{\partial\sigma}\\
&=\lambda x(\sigma,\tau)-\frac{\beta x(\sigma,\tau)}{|I_{r_c}(\sigma,\tau)|}\int_{I_{r_c}(\sigma,\tau)}v(\omega,\tau)\,d\omega\\
&\quad-\frac{\rho x(\sigma,\tau)}{|I_{2r_c}(\sigma,\tau)|}\int_{I_{2r_c}(\sigma,\tau)}1-x(\omega,\tau)\,d\omega-x(\sigma,\tau)[\lambda x(\sigma,\tau)\\
&\quad-\delta y(\sigma,\tau)-\mu(1-x(\sigma,\tau)-y(\sigma,\tau)],
\end{aligned}
\tag{47}
$$

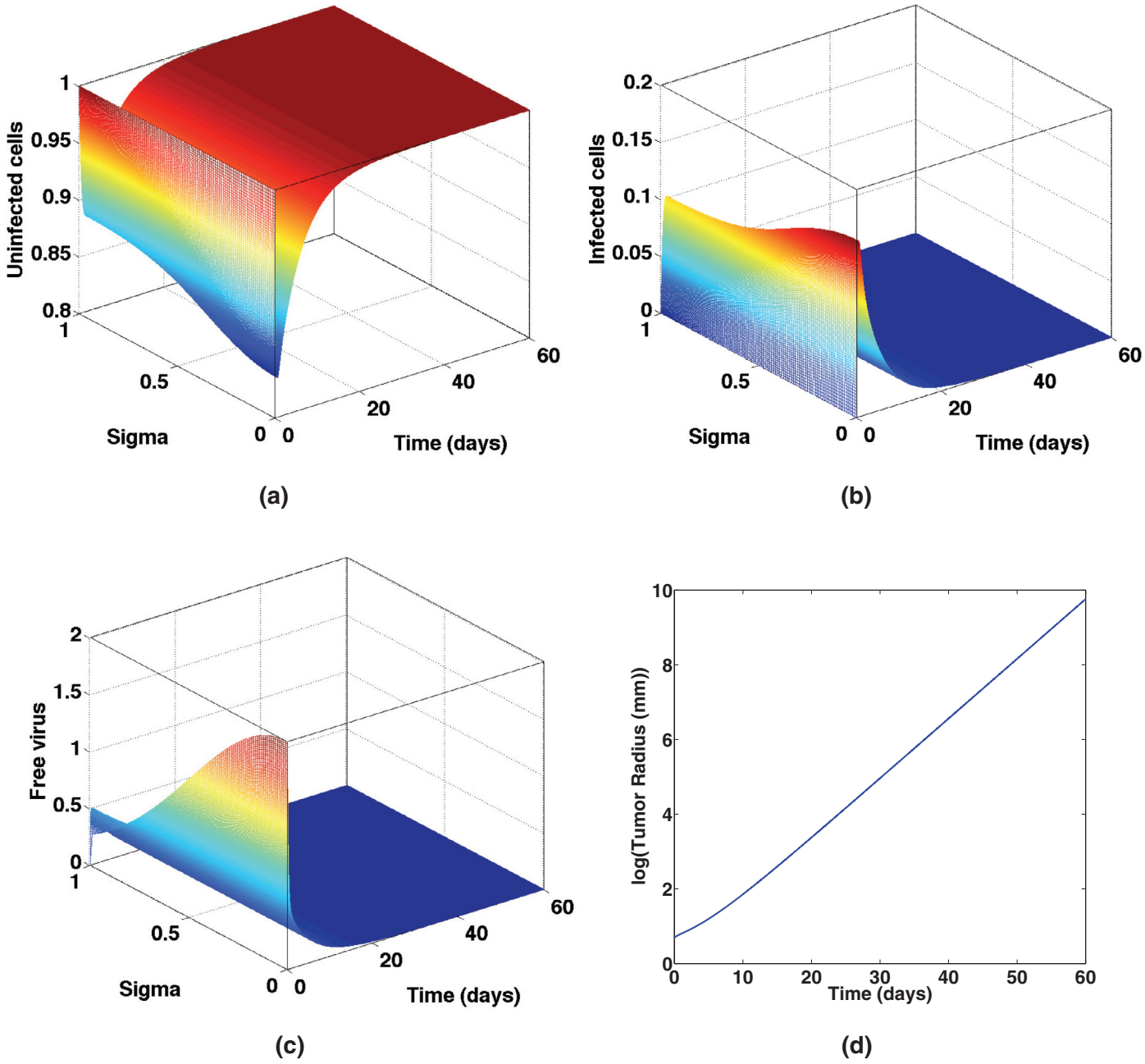

Fig. 4. Convergence to the infection-free equilibrium $(1, 0, 0)$ for $\tilde{\rho} = 0.1$ and $N = 30$. Nondimensional values for (a) uninfected tumor cells, (b) infected tumor cells, and (c) free virus are plotted versus time and σ, the scaled distance from the tumor center. (d) The tumor radius demonstrates exponential growth.

$$\frac{\partial y(\sigma,\tau)}{\partial \tau} + \left[-\frac{\sigma}{R(\tau)}\frac{dR(\tau)}{d\tau} + \frac{u(\sigma,\tau)}{R(\tau)}\right]\frac{\partial y(\sigma,\tau)}{\partial \sigma} = \frac{\beta x(\sigma,\tau)}{|I_{r_c}(\sigma,\tau)|}\int_{I_{r_c}(\sigma,\tau)} v(\omega,\tau)\,d\omega - (\rho+\delta)y(\sigma,\tau) - y(\sigma,\tau)[\lambda x(\sigma,\tau) - \delta y(\sigma,\tau) - \mu(1 - x(\sigma,\tau) - y(\sigma,\tau)], \tag{48}$$

$$\frac{\partial v(\sigma,\tau)}{\partial \tau} - \frac{\sigma}{R(\tau)}\frac{dR(\tau)}{d\tau}\frac{\partial v(\sigma,\tau)}{\partial \sigma} - \frac{\kappa}{R^2(\tau)}\frac{1}{\sigma^2}\frac{\partial}{\partial \sigma}\left(\sigma^2\frac{\partial v(\sigma,\tau)}{\partial \sigma}\right) = \frac{\delta}{|J_{r_c}(\sigma,\tau)|}\int_{I_{r_c}(\sigma,\tau)}\left[r_c^2 - R^2(\tau)(\sigma-\omega)^2\right]y(\omega,\tau)\,d\omega + \frac{\alpha}{|I_{r_c}(\sigma,\tau)|}\int_{I_{r_c}(\sigma,\tau)} 1 - x(\omega,\tau)\,d\omega - \gamma v(\sigma,\tau), \tag{49}$$

$$u(\sigma,\tau) = \frac{R(\tau)}{\sigma^2}\int_0^\sigma \omega^2[-\mu + (\lambda+\mu)x(\omega,\tau) + (\mu-\delta)y(\omega,\tau)]\,d\omega, \tag{50}$$

$$\frac{dR(\tau)}{d\tau} = u(1,\tau). \tag{51}$$

The boundary and initial conditions remain as given in (21)–(26).

4.3. Numerical method

A finite difference numerical scheme was formulated for the system (47)–(51), (21)–(26) adapted from the method formulated by Wang and Tian for a simpler virotherapy model [15]. In brief, the second order Adams–Bashforth method is used to calculate R at each time step; the trapezoidal rule is used for u. The Leapfrog scheme, which assumes central differences in time and space, is used to advance $\bar{x}$

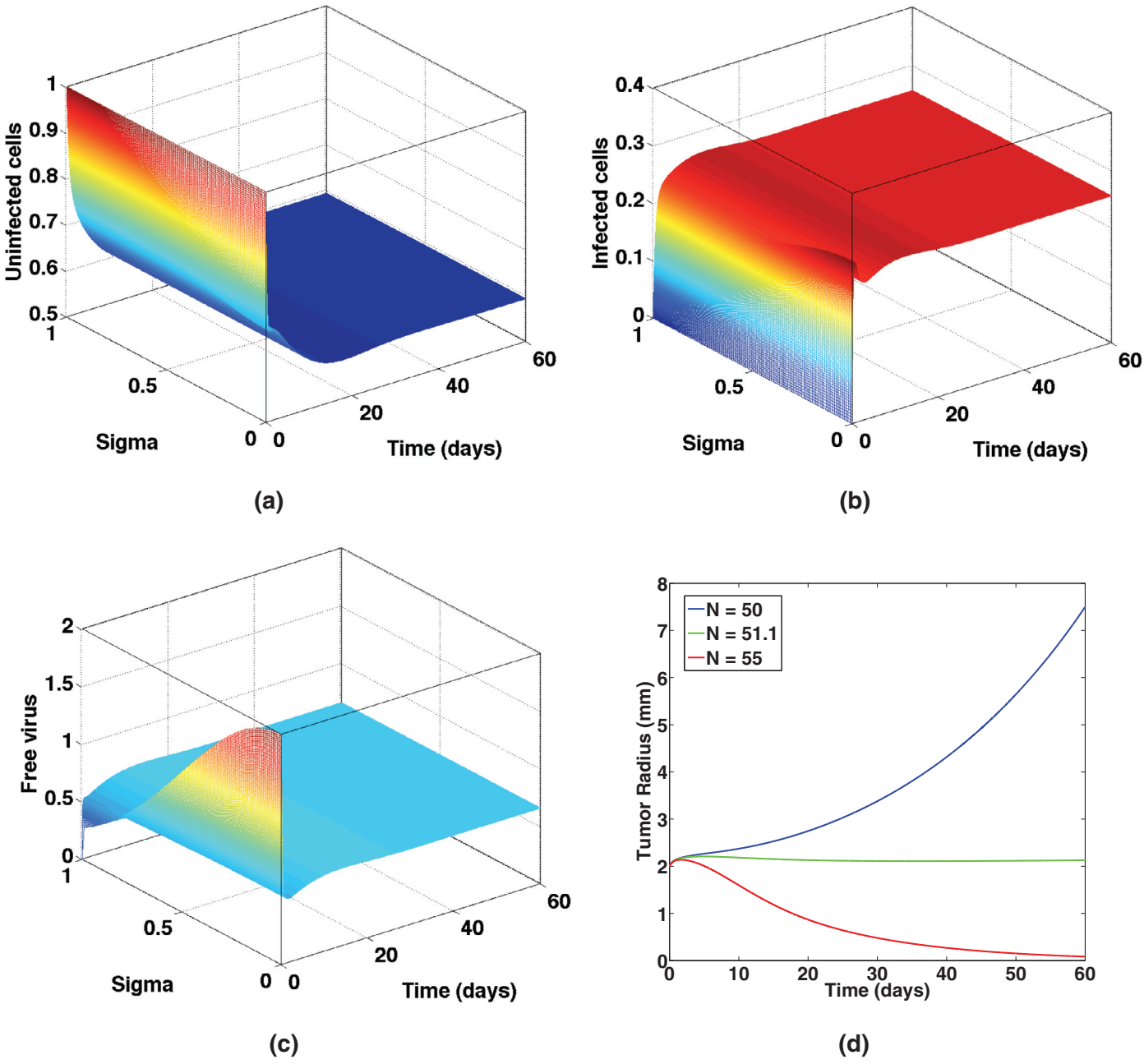

Fig. 5. Convergence to the endemic equilibrium for $\bar{\rho} = 0.1$. Nondimensional values for (a) uninfected tumor cells, (b) infected tumor cells, and (c) free virus are plotted versus time and σ, the scaled distance from the tumor center, for $N = 55$. (d) The tumor radius demonstrates exponential growth, stabilization, and exponential decay, respectively, for $N = 50$, $N = 51.1$, and $N = 55$.

and $\bar{y}$. We employ the second-order implicit backward differentiation formula method in time and central differences in space to solve the parabolic $\bar{v}$ equation at each time step. This requires a standard tridiagonal matrix algorithm [28]. Our method also includes computation of the definite integrals at each time step which are approximated by the trapezoidal rule. Further details of the method are presented in [15].

We assume that the oncolytic virus is injected into the center of the tumor at time $t = 0$. Therefore, we model the initial virus profile by $\bar{v}(\sigma, 0) = a \exp(\frac{-\sigma^2}{2b^2})$ where $a = 2$ and $b = 0.5$. The other initial conditions are given by $\bar{x}(\sigma, 0) = 1$, $\bar{y}(\sigma, 0) = 0$, and $R(0) = 2$ mm; i.e., we assume that initially there are no infected cells.

4.4. Integral terms and spatial homogeneity

Our numerical method maintains the averaging property of the nonlocal integral terms. Therefore, solutions with a spatially homogeneous initial condition should remain spatially homogeneous; this behavior was confirmed by numerical simulations (not shown). Furthermore, all simulations attempted resulted in convergence to spatially homogeneous solutions (e.g. Fig. 4). Hence, these solutions will asymptotically satisfy the corresponding ordinary differential equations system, i.e. Eqs. (16)–(20) with $\tilde{x} = \bar{x}(\tau)$, $\tilde{y} = \bar{y}(\tau)$, and $\tilde{v} = \bar{v}(\tau)$. Global stability analysis of the ODE system will be considered in other work.

Please cite this article as: K. Jacobsen, S. S. Pilyugin, Analysis of a mathematical model for tumor therapy with a fusogenic oncolytic virus, Mathematical Biosciences (2015), http://dx.doi.org/10.1016/j.mbs.2015.02.009

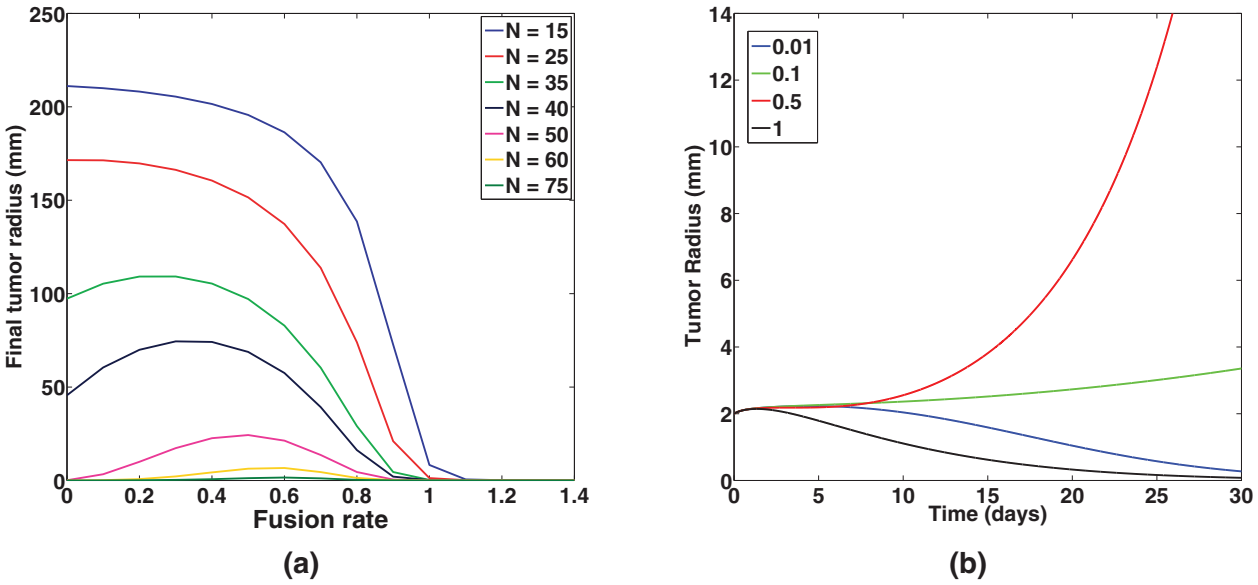

Fig. 6. Effects of rate of fusion, $\bar{\rho}$, on tumor growth. (a) Final tumor radius (i.e. at $\tau = 30$ days) plotted versus fusion rate, $\bar{\rho}$, for varying values of viral burst size, N. Final tumor radius decreases as N increases but is not monotone with respect to $\bar{\rho}$ for larger values of N. (b) Tumor radius versus time for $N = 50$ and varying values of $\bar{\rho}$. The tumor radius decays for small and large values of $\bar{\rho}$ but grows for intermediate values of $\bar{\rho}$.

We also compared the numerical method described in Section 4 with one that replaces the integral terms with corresponding local mass action terms. Even with non-spatially homogenous initial conditions, density plots showed no perceptible difference between the two methods. However, the original method is more computationally expensive so the remaining simulations use the method with mass action.

4.5. Tumor growth behavior

In the spatially homogeneous case, it follows from Eqs. (50) and (51) that growth of the tumor radius is determined by the equation

$$\dot{R} = \frac{R}{3}[(\lambda+\mu)\bar{x} + (\mu-\delta)\bar{y} - \mu].$$

Suppose a solution of system (47)–(51), (21)–(26) converges to a spatially homogeneous solution $(\tilde{X}, \tilde{Y}, \tilde{V})$. Then, long-term tumor growth is exponential with the rate of growth or decay determined by

$$\tilde{F} := \frac{1}{3}[(\lambda+\mu)\tilde{X} + (\mu-\delta)\tilde{Y} - \mu].$$

If a solution converges to the infection-free equilibrium (IFE) $(1, 0, 0)$, then the tumor is predicted to eventually grow exponentially with growth constant $\tilde{F} = \lambda/3$. Indeed, with parameter values $\bar{\rho} = 0.1$ and $N = 30$ the numerical solution converges to the IFE (Fig. 4). Furthermore, linear regression of the log plot of R (Fig. 4(d)) for $50 \le \tau \le 60$ reveals a growth rate of 0.16. Recall that $\lambda = 0.48$, so the predicted growth rate is $\tilde{F} = \lambda/3 = 0.16$, thus confirming the accuracy of our numerical method.

4.5.1. Effects of viral burst size, N

A more interesting case is when a solution converges to the endemic equilibrium. Although there is a positive density of uninfected cancer cells, the long-term behavior of the tumor radius may be exponential growth or decay, depending on the sign of $\tilde{F}$. In Fig. 5(a)–(c) the parameters include $\bar{\rho} = 0.1$ and $N = 55$; in this case, $\tilde{F} = -0.058$ and the tumor decays exponentially (Fig. 5(d)). If, instead, $N = 50$ with other parameters equal, the tumor grows exponentially (Fig. 5(d)) since $\tilde{F} = 0.0311$. We are also able to isolate the special boundary case with $N = 51.1$ where $\tilde{F} \approx 0$ and the tumor radius stabilizes at approximately 2.1 mm (Fig. 5(d)). The effect demonstrated in Fig. 5(d) that long-term tumor radius will decrease with increasing viral burst size (N) is expected; larger burst sizes correspond to more virulent viruses and, hence, more effective virotherapy.

4.5.2. Effects of the rate of fusion, $\bar{\rho}$

The effect of increasing the rate of fusion ($\bar{\rho}$), on the other hand, is less obvious. In Fig. 6(a) we plot the final tumor radius, i.e. at $\tau = 30$ days, for a range of values of $\bar{\rho}$ and N. When N is small the final tumor radius decreases with increasing $\bar{\rho}$ as expected. However, for larger values of N the final tumor radius is not monotone with respect to $\bar{\rho}$. Indeed, when $N = 50$ for example, the final tumor radius increases until $\bar{\rho} = 0.5$ and then decreases thereafter. Fig. 6(b) shows the evolution of the tumor radius over time for $N = 50$ and four different values of $\bar{\rho}$. With a low rate of fusion, i.e. $\bar{\rho} = 0.01$, the tumor decays. However, when $\bar{\rho}$ increases to 0.1 and 0.5, $\tilde{F}$ has changed sign and the tumor radius grows exponentially. When the rate of fusion is sufficiently large, such as with $\bar{\rho} = 1$, long-term radius behavior is again exponential decay. Furthermore, the decay rate corresponding to $\bar{\rho} = 1$ is of greater magnitude compared to the rate when $\bar{\rho} = 0.01$, indicating that rapid fusion can potentially lead to quicker reduction in tumor size, an important clinical consideration.

We provide one possible explanation for this nonmonotonic behavior. It may be that, for small $\bar{\rho}$, the lysis mechanism dominates and can be sufficient to control the tumor. With slightly higher $\bar{\rho}$, fusion is fast enough to deplete the local availability of uninfected tumor cells leaving nearby viral particles ineffective, but is not large enough to control tumor growth. Finally, when $\bar{\rho}$ becomes sufficiently large, fusion can quickly occur throughout the entire tumor volume leading to exponential decay.

5. Discussion

In the present work a hyperbolic–parabolic PDE system with nonlocal integrals was formulated to model tumor therapy with a fusogenic oncolytic virus. Existence and uniqueness of global solutions was proven using a nested application of the contraction mapping theorem. Numerical simulations provided predictions of tumor

Please cite this article as: K. Jacobsen, S. S. Pilyugin, Analysis of a mathematical model for tumor therapy with a fusogenic oncolytic virus, Mathematical Biosciences (2015), http://dx.doi.org/10.1016/j.mbs.2015.02.009

growth, decay, or stabilization depending on viral burst size and rate of fusion. The model predicts that long-term tumor radius decreases with increasing viral burst size but, interestingly, the effect of the rate of fusion on the tumor radius is nonmonotonic. The model was parameterized in this work for a fusogenic oncolytic herpes simplex virus. However, with further experimental data, the well-posed model could be tailored to other viruses with differing dominant viral spread mechanisms. Data is particularly needed in order to better estimate the rate of fusion which was shown to be an important factor in determining success or failure of therapy. Further analysis of the mechanism of syncytia formation on tumor-virus dynamics could provide insights to improve the efficacy of oncolytic virotherapy.

Acknowledgments

We thank the anonymous referees for their helpful comments. Many thanks also to Avner Friedman for valuable discussions. K. Jacobsen was supported in part by the Mathematical Biosciences Institute and the National Science Foundation under Grant No. DMS-0931642. The majority of this work was done when she was completing her Ph.D. thesis at the University of Florida.

References

[1] K. Parato, D. Senger, P. Forsyth, J. Bell, Recent progress in the battle between oncolytic viruses and tumours, Nat. Rev. Cancer 5 (12) (2005) 965–976. 10.1038/nrc1750
[2] O. Ebert, K. Shinozaki, C. Kournioti, M. Park, A. García-Sastre, S. Woo, Syncytia induction enhances the oncolytic potential of vesicular stomatitis virus in virotherapy for cancer, Cancer Res. 64 (9) (2004) 3265.
[3] E. Kelly, S. Russell, History of oncolytic viruses: genesis to genetic engineering, Mol. Ther. 15 (4) (2007) 651–659.
[4] A. Bateman, K. Harrington, T. Kottke, A. Ahmed, A. Melcher, M. Gough, E. Linardakis, D. Riddle, A. Dietz, C. Lohse, et al., Viral fusogenic membrane glycoproteins kill solid tumor cells by nonapoptotic mechanisms that promote cross presentation of tumor antigens by dendritic cells, Cancer Res. 62 (22) (2002) 6566.
[5] A. Bateman, F. Bullough, S. Murphy, L. Emiliusen, D. Lavillette, F. Cosset, R. Cattaneo, S. Russell, R. Vile, Fusogenic membrane glycoproteins as a novel class of genes for the local and immune-mediated control of tumor growth, Cancer Res. 60 (6) (2000) 1492.
[6] X. Fu, X. Zhang, Potent systemic antitumor activity from an oncolytic herpes simplex virus of syncytial phenotype, Cancer Res. 62 (8) (2002) 2306.
[7] C. McDonald, C. Erlichman, J. Ingle, G. Rosales, C. Allen, S. Greiner, M. Harvey, P. Zollman, S. Russell, E. Galanis, A measles virus vaccine strain derivative as a novel oncolytic agent against breast cancer, Breast Cancer Res. Treat. 99 (2) (2006) 177–184. 10.1007/s10549-006-9200-5
[8] E.H. Lin, C. Salon, E. Brambilla, D. Lavillette, J. Szecsi, F.L. Cosset, J.L. Coll, Fusogenic membrane glycoproteins induce syncytia formation and death in vitro and in vivo: a potential therapy agent for lung cancer, Cancer Gene Ther. 17 (4) (2010) 256–265. 10.1038/cgt.2009.74
[9] M. Nakamori, X. Fu, R. Rousseau, S. Chen, X. Zhang, Destruction of nonimmunogenic mammary tumor cells by a fusogenic oncolytic herpes simplex virus induces potent antitumor immunity, Mol. Ther. 9 (5) (2004) 658–665. 10.1016/j.ymthe.2004.02.019
[10] J. Wu, H. Byrne, D. Kirn, L. Wein, Modeling and analysis of a virus that replicates selectively in tumor cells, Bull. Math. Biol. 63 (4) (2001) 731–768.
[11] J.T. Wu, D.H. Kirn, L.M. Wein, Analysis of a three-way race between tumor growth, a replication-competent virus and an immune response, Bull. Math. Biol. 66 (4) (2003) 605–625. 10.1016/j.bulm.2003.08.016
[12] L. Wein, J. Wu, D. Kirn, Validation and analysis of a mathematical model of a replication-competent oncolytic virus for cancer treatment: implications for virus design and delivery, Cancer Res. 63 (6) (2003) 1317–1324.
[13] A. Friedman, Y. Tao, Analysis of a model of a virus that replicates selectively in tumor cells, J. Math. Biol. 47 (5) (2003) 391–423.
[14] Y. Tao, Q. Guo, The competitive dynamics between tumor cells, a replication-competent virus and an immune response, J. Math. Biol. 51 (1) (2005) 37–74. 10.1007/s00285-004-0310-6
[15] J. Wang, J. Tian, Numerical study for a model of tumor virotherapy, Appl. Math. Comput. 196 (1) (2008) 448–457.
[16] Ž. Bajzer, T. Carr, K. Josić, S. Russell, D. Dingli, Modeling of cancer virotherapy with recombinant measles viruses, J. Theor. Biol. 252 (1) (2008) 109–122.
[17] D. Dingli, C. Offord, R. Myers, K. Peng, T.W. Carr, K. Josic, S. Russell, Z. Bajzer, Dynamics of multiple myeloma tumor therapy with a recombinant measles virus, Cancer Gene Ther. 16 (12) (2009) 873–882.
[18] M. Biesecker, J. Kimn, H. Lu, D. Dingli, Ž. Bajzer, Optimization of virotherapy for cancer, Bull. Math. Biol. 72 (2) (2010) 469–489.
[19] C. Reis, J. Pacheco, M. Ennis, D. Dingli, In silico evolutionary dynamics of tumour virotherapy, Integr. Biol. 2 (1) (2010) 41–45. 10.1039/b917597k
[20] H. Landau, Heat conduction in a melting solid, Quart. Appl. Math 8 (1) (1950) 81–94.
[21] C. Chicone, Ordinary Differential Equations with Applications, vol. 34, 2nd ed., Springer, 2006.
[22] A. Friedman, Partial Differential Equations of Parabolic Type, vol. 196, Prentice-Hall, Englewood Cliffs, NJ, 1964.
[23] A. Leung, Systems of Nonlinear Partial Differential Equations: Applications to Biology and Engineering, Kluwer Academic Publishers Boston, 1989.
[24] A. Friedman, J. Tian, G. Fulci, E. Chiocca, J. Wang, Glioma virotherapy: effects of innate immune suppression and increased viral replication capacity, Cancer Res. 66 (4) (2006) 2314.
[25] G. Fulci, L. Breymann, D. Gianni, K. Kurozomi, S. Rhee, J. Yu, B. Kaur, D. Louis, R. Weissleder, M. Caligiuri, et al., Cyclophosphamide enhances glioma virotherapy by inhibiting innate immune responses, Proc. Nat. Acad. Sci. 103 (34) (2006) 12873–12878.
[26] K. Kurozumi, J. Hardcastle, R. Thakur, J. Shroll, M. Nowicki, A. Otsuki, E.A. Chiocca, B. Kaur, Oncolytic HSV-1 infection of tumors induces angiogenesis and upregulates cyr61, Mol. Ther. 16 (8) (2008) 1382–1391.
[27] S. Nii, C. Morgan, H.M. Rose, Electron microscopy of herpes simplex virus: Ii. sequence of development, J. Virol. 2 (5) (1968) 517.
[28] L. Thomas, Elliptic problems in linear difference equations over a network, Watson Sci. Comput. Lab. Rept., Columbia University, New York, 1949.